

Theoretical predictions for α -decay chains of $^{290-298}_{118}\text{Og}$ isotopes using a finite-range nucleon-nucleon interaction

M. Ismail¹ and A. Adel^{1,2,*}¹*Physics Department, Faculty of Science, Cairo University, Giza, Egypt*²*Physics Department, College of Science, Majmaah University, Zulfi, Saudi Arabia*

(Received 13 December 2017; revised manuscript received 15 February 2018; published 4 April 2018)

The α -decay half-lives of the recently synthesized superheavy nuclei (SHN) are investigated by employing the density dependent cluster model. A realistic nucleon-nucleon (NN) interaction with a finite-range exchange part is used to calculate the microscopic α -nucleus potential in the well-established double-folding model. The calculated potential is then implemented to find both the assault frequency and the penetration probability of the α particle by means of the Wentzel-Kramers-Brillouin (WKB) approximation in combination with the Bohr-Sommerfeld quantization condition. The calculated values of α -decay half-lives of the recently synthesized Og isotopes and its decay products are in good agreement with the experimental data. Moreover, the calculated values of α -decay half-lives have been compared with those values evaluated using other theoretical models, and it was found that our theoretical values match well with their counterparts. The competition between α decay and spontaneous fission is investigated and predictions for possible decay modes for the unknown nuclei $^{290-298}_{118}\text{Og}$ are presented. We studied the behavior of the α -decay half-lives of Og isotopes and their decay products as a function of the mass number of the parent nuclei. We found that the behavior of the curves is governed by proton and neutron magic numbers found from previous studies. The proton numbers $Z = 114, 116, 108, 106$ and the neutron numbers $N = 172, 164, 162, 158$ show some magic character. We hope that the theoretical prediction of α -decay chains provides a new perspective to experimentalists.

DOI: [10.1103/PhysRevC.97.044301](https://doi.org/10.1103/PhysRevC.97.044301)

I. INTRODUCTION

Among various decay modes, α decay is the prominent one for heavy and superheavy nuclei (SHN) [1,2]. It probes much unique insights into the nuclear structure [3–10]. The identification of superheavy nuclei is mainly obtained via the observation of α -decay chains from an unknown parent nucleus to a known daughter nucleus [11–13]. Recently, extensive studies have been devoted to study the decay properties of superheavy nuclei [14–34].

The synthesis of superheavy nuclei [35–37] has attracted much attention in recent years and raised the question about the upper limit of the periodic table. Accurate predictions for the α -decay half-lives of SHN are urgently required for the synthesis of new elements. At the present time attempts are being made to synthesize the superheavy nucleus $^{296}_{118}\text{Og}$ [38], which would be the heaviest nucleus to date, situated at the border of the known nuclear chart. Two fusion-evaporation mechanisms are usually used to synthesize SHN, namely, the cold fusion reactions using ^{208}Pb or ^{209}Bi targets with different projectiles [39] and the hot fusion reactions using ^{48}Ca projectiles bombarding actinide targets [40]. Using the cold fusion reaction [39], elements with $Z = 107–112$ have been synthesized at GSI, Darmstadt in Germany. The most challenging cold-fusion experiment, which used a ^{209}Bi target and ^{70}Zn projectile, ran for nine years at the RIKEN research institute in Japan

which resulted in the observation of three decay chains of the isotope $^{278}_{113}\text{Nh}$ [41]. Elements with $Z = 113–118$ have been synthesized at the Joint Institute for Nuclear Research-Flerov Laboratory of Nuclear Reactions (JINR-FLNR), Dubna using the hot fusion reaction [40]. One of the significant outcomes of these measurements is the increased stability of SHN when approaching $N = 184$. The heaviest neutron-rich nuclei in the vicinity of the closed spherical shells $Z = 114$ (or possibly 120, 122, or 126) and $N = 184$ were expected to mark a considerable increase in nuclear stability, similar to the effect of closed shells on the stability of the doubly magic ^{208}Pb nucleus.

The dominant decay modes for SHN are α decay and spontaneous fission (SF) that determine the stability of SHN and represent the experimental signatures for their identification [1,2]. However, the identification of the new isotopes still poses a problem because their α -decay chains terminate by SF before reaching the known region of the nuclear chart. Thus, the theoretical predictions about the stability of Og isotopes against α decay, SF, and the competition between them are useful in interpreting the experimental results. Theoretically, α decay is a quantum tunneling effect. It is treated conventionally in the framework of the Gamow model [42] assuming a sub-barrier penetration of α particles through the Coulomb barrier, caused by interactions between α particles and the daughter nucleus. α -decay studies from heavy and superheavy nuclei are performed using various effective theoretical approaches, such as the generalized liquid-drop model [43], the fission-like model [44], and the density-dependent cluster model [45].

*ahmedadel@sci.cu.edu.eg; aa.ahmed@mu.edu.sa

Santhosh and Nithya have made systematic studies of the decay properties of superheavy nuclei within the Coulomb and proximity potential model [14–20].

Several empirical formulas are proposed to predict α -decay half-lives, such as the Viola-Seaborg-Sobiczewski (VSS) formula [46,47], Ni-Ren-Dong-Xu (NRDX) formula [48], Royer formula [49], Sobiczewski-Parkhomenko (SP) formula [50], modified Brown formula (mB1) [51], Horoi formula [52], and the semiempirical formula based on fission theory (SemFIS2) [53]. Using 20 mass models and 18 empirical formulas, Wang *et al.* [54] presented systematic calculations of α -decay energies and half-lives of SHN with $Z \geq 100$. They found that the best suitable formula, among 18 formulas, to predict α -decay half-lives is the SemFIS2 [53] formula, while the WS4 mass model [55] is the most accurate mass model to reproduce the experimental Q_α values of the SHN.

An interesting aspect in α -decay is how to describe the preformation of the α cluster inside the parent nucleus, which is quite complicated due to its nuclear many-body nature [56]. This factor is considered to carry most information of nuclear structure, which is essential to understand how a clustering happens in heavy nuclei [10,57–59]. The α preformation factor or the so-called spectroscopic factor S_α represents the probability of existence of an α cluster inside the parent nucleus as a recognizable entity before its emission [60]. The α -preformation factor (S_α) can be estimated using different theoretical approaches. For example, Varga *et al.* [56] investigated the ^{212}Po nucleus of only four valence nucleons above a core of closed shells by using the R matrix and the combined cluster-shell model within the effective nucleon-nucleon interaction. This microscopic calculations were performed due to the simplicity of structure for ^{212}Po , and it would be very difficult to apply a fully microscopic description of S_α to nuclei of many valence nucleons and high shell-model configuration states. Many works assumed S_α to be a constant for a certain kind of nuclei (even-even, odd-A, odd-odd) [61] through minimizing the deviation between theoretical and experimental decay widths. One can roughly estimate the S_α factors through dividing the experimental decay width by the computed value [10]. The recently proposed cluster formation model (CFM) [57,62–64] suggests that the α -preformation factor can be calculated in terms of the α -cluster formation energy based on the binding energy differences of the participating nuclides. A realistic result was obtained for the value of the α -preformation factor of ^{212}Po from the CFM, which is consistent with the value reported by Varga *et al.* [56].

In the present study, we systematically study α -decay half-lives of the recently observed SHN and give predictions of various α -decay chains of the isotopes of the superheavy element oganesson (Og) with $Z = 118$, which may be useful for the current experiments at FLNR in Dubna [2,38]. We discuss the competition between α decay, calculated from five different approaches, and spontaneous fission for nine different isotopes of element Og. Some of these isotopes are unknown and the present study predicts their decay modes. The present work uses a realistic nucleon-nucleon (NN) interaction with a finite-range exchange part [65–68] to calculate the microscopic α -nucleus potential in the well-established double-folding model [69]. The α -decay half-lives are investigated by

employing the density dependent cluster model [45,70] in the framework of the Wentzel-Kramers-Brillouin (WKB) approximation in combination with the Bohr-Sommerfeld quantization condition [71]. Two methods for calculating the preformation probabilities are used. The first one simply uses a constant value of S_α for a certain kind of nuclei, which is frequently used in previous studies [45,61]. The other method is based on the recently proposed cluster formation model (CFM) [57,62–64], which gives realistic α preformation factors. It is hoped that the present study can be a helpful reference for microscopic calculation in the future.

The outline of the paper is as follows. In Sec. II a description of the microscopic nuclear and Coulomb potentials between the α and daughter nuclei is given. The methods for determining the decay width, the penetration probability, the assault frequency, and the preformation probability are also presented. In Sec. III, the calculated results are discussed. Finally, Sec. IV gives a brief conclusion.

II. THEORETICAL FRAMEWORK

In the performed cluster models, the α particle is considered to be formed with a definite probability as an individual cluster inside the parent nucleus at the preliminary stage. Once formed, it will try to emit, leaving the daughter nucleus behind. The α -decay partial half-lifetime, $T_{1/2}$, of the parent nucleus is given in terms of the α -decay width, Γ , as

$$T_{1/2} = \frac{\hbar \ln 2}{\Gamma}. \quad (1)$$

The absolute α -decay width is mainly determined by the barrier penetration probability (P_α), the assault frequency (ν), and the preformation probability, the spectroscopic factor of the α -cluster inside the parent nucleus (S_α): $\Gamma = \hbar S_\alpha \nu P_\alpha$. The barrier penetration probability, P_α , could be calculated as the barrier transmission coefficient of the well-know Wentzel-Kramers-Brillouin (WKB) approximation [45,72], which works well at energies well below the barrier:

$$P_\alpha = \exp\left(-2 \int_{R_2}^{R_3} dr \sqrt{\frac{2\mu}{\hbar^2} |V_T(r) - Q_\alpha|}\right) \quad (2)$$

Here μ is the reduced mass and Q_α is the Q value of the α decay. R_i ($i = 1, 2, 3$) are the three turning points for the α -daughter potential barrier where $V_T(r)|_{r=R_i} = Q_\alpha$.

The assault frequency of the α particle, ν , can be expressed as the inverse of the time required to traverse the distance back and forth between the first two turning points, R_1 and R_2 , as [72]

$$\nu = T^{-1} = \frac{\hbar}{2\mu} \left[\int_{R_1}^{R_2} \frac{dr}{\sqrt{\frac{2\mu}{\hbar^2} |V_T(r) - Q_\alpha|}} \right]^{-1} \quad (3)$$

The total interaction potential of the α -core system comprises the nuclear and the Coulomb potentials plus the

centrifugal part, and is given by [45,70,72]

$$V_T(R) = \lambda V_N(R) + V_C(R) + \frac{\hbar^2}{2\mu} \frac{(\ell + \frac{1}{2})^2}{R^2}, \quad (4)$$

where the renormalization factor λ is the depth of the nuclear potential, R is the separation distance between the mass center of the α particle and the mass center of the core, and ℓ is the angular momentum carried by the α particle. The latter term in Eq. (4) represents the Langer modified centrifugal potential [73]. The preceding modification from $\ell(\ell + 1) \rightarrow (\ell + 1/2)^2$ is essential to ensure the correct behavior of the scattered radial wave function near the origin [72,74]. We use the minimum values of possible angular momenta; the α particle can transfer any value of the angular momentum according to the following spin-parity selection rule:

$$|J_i - J_f| \leq \ell \leq |J_i + J_f| \quad \text{and} \quad \frac{\pi_f}{\pi_i} = (-1)^\ell, \quad (5)$$

where J_i , π_i and J_f , π_f are the spin and parity of parent and daughter nuclei, respectively. ℓ is considered zero whenever the spin and parity of any of the participating nuclei are not measured.

The renormalization factor λ , introduced to the nuclear part of the folding potential based on the M3Y interaction, is not an adjustable parameter, but it is determined separately for each decay by applying the Bohr-Sommerfeld quantization condition as described in Ref. [45]

$$\int_{R_1}^{R_2} dr \sqrt{\frac{2\mu}{\hbar^2} |V_T(r) - Q_\alpha|} = (G - \ell + 1) \frac{\pi}{2} \quad (6)$$

where the global quantum number $G = 20$ ($N > 126$) and $G = 18$ ($82 < N \leq 126$) [45]. In Ref. [72], the half-lives are found to be sensitive to the implementation of this condition in the WKB approach, which fixes the depth of the double-folding nuclear potential λ .

The nuclear part of the potential $V_N(R)$ consists of two terms, the direct $V_D(R)$ and the exchange $V_{Ex}(R)$ terms, and is given by

$$V_N(R) = V_D(R) + V_{Ex}(R) \quad (7)$$

The direct part of the interaction between two colliding nuclei and the equation describing the Coulomb interaction have similar forms involving only diagonal elements of the density matrix [69]:

$$V_D(R) = \int d\vec{r}_1 \int d\vec{r}_2 \rho_\alpha(\vec{r}_1) v_D(s) \rho_d(\vec{r}_2), \quad (8)$$

where s is the relative distance between a constituent nucleon in the α particle and one in the daughter nucleus. $\rho_\alpha(r_1)$ and $\rho_d(\vec{r}_2)$ are, respectively, the density distributions of the α particle and the residual daughter nucleus as described in Ref. [45].

The exchange part involves nondiagonal elements of the density matrix and the wave number $k(R)$ associated with the relative motion of the colliding nuclei. According to Ref. [67], one easily obtains the self-consistent and local exchange

potential V_{Ex} as

$$V_{Ex}(R) = 4\pi \int_0^\infty ds s^2 v_{Ex}(s) j_0[k(R)s/M] \\ \times \int d\vec{y} \rho_d(|\vec{y} - \vec{R}|) \hat{j}_1[k_{\text{eff}}(|\vec{y} - \vec{R}|)s] \\ \times \rho_\alpha(y) \exp\left(-\frac{s^2}{4b_\alpha^2}\right) \quad (9)$$

Here $k(R)$ is the relative motion momentum given by [75]

$$k^2(R) = \frac{2\mu}{\hbar^2} [E_{\text{c.m.}} - V_N(R) - V_C(R)], \quad (10)$$

where $E_{\text{c.m.}}$ is the center-of-mass energy. $V_N(R)$ and $V_C(R)$ are the total nuclear and Coulomb potentials, respectively.

The local Fermi momentum $k_{\text{eff}}(r)$ is given by [67]

$$k_{\text{eff}}(r) = \left\{ \frac{5}{3\rho(r)} \left[\tau(r) - \frac{1}{4} \nabla^2 \rho(r) \right] \right\}^{1/2}. \quad (11)$$

The kinetic energy density is then given by

$$\tau(r) = \frac{3}{5} \left(\frac{3\pi^2}{2} \right)^{2/3} \rho(r)^{5/3} + \frac{1}{3} \nabla^2 \rho(r) + \frac{1}{36} \frac{|\vec{\nabla} \rho(r)|^2}{\rho(r)}. \quad (12)$$

The exchange potential, Eq. (9), can then be evaluated by an iterative procedure which converges very fast.

The realistic M3Y-Paris effective NN interaction is used in our present calculations and it has the form [69,76,77]

$$v_D(s) = \left[11061.625 \frac{e^{-4s}}{4s} - 2537.5 \frac{e^{-2.5s}}{2.5s} \right], \quad (13)$$

$$v_{Ex}(s) = \left[-1524.25 \frac{e^{-4s}}{4s} - 518.75 \frac{e^{-2.5s}}{2.5s} \right. \\ \left. - 7.8474 \frac{e^{-0.7072s}}{0.7072s} \right]. \quad (14)$$

The obtained α -daughter interaction potential is employed to compute the barrier penetrability, Eq. (2), and the assault frequency, Eq. (3), which are used in turn to obtain the decay half-life time. The α -decay preformation factor, S_α , used in the present calculations, is derived from the cluster formation model (CFM) [57,62–64].

On the basis of the cluster formation model (CFM) [57,62–64], a parent nucleus of total energy E exhibits behaviors of N_s different clusterization states. The initial state, Ψ , of the parent nucleus can be defined as the superposition of all possible clusterization states Ψ_i with the amplitude a_i subjected to orthonormality, and the total Hamiltonian for the system H can be represented by the summation of corresponding clusterization Hamiltonians H_i :

$$\Psi = \sum_i^{N_s} a_i \Psi_i, \quad (15)$$

$$H = \sum_i^{N_s} H_i. \quad (16)$$

TABLE I. Comparison of α -decay half-lives using the double-folding model with constant preformation factor, $T_{1/2}^{\text{calc1}}$; the Viola-Seaborg-Sobiczewski (VSS) formula [46,47], $T_{1/2}^{\text{VSS}}$; the modified Brown (mB1) formula [51], $T_{1/2}^{\text{mB1}}$; and the semiempirical formula [53], $T_{1/2}^{\text{SemFIS2}}$ with the recent experimental values [37]. The calculations are done for zero angular momentum transfers.

| Parent nuclei | $Q_{\alpha}^{\text{expt.}}$ (MeV) | $T_{1/2}^{\text{expt.}}$ | $T_{1/2}^{\text{calc1}}$ | $T_{1/2}^{\text{VSS}}$ | $T_{1/2}^{\text{mB1}}$ | $T_{1/2}^{\text{SemFIS2}}$ |
|-------------------------|-----------------------------------|-----------------------------|--------------------------|------------------------|------------------------|----------------------------|
| $^{294}_{118}\text{Og}$ | 11.82 ± 0.06 | $0.69^{+0.64}_{-0.22}$ ms | 0.65 ms | 0.60 ms | 0.57 ms | 0.96 ms |
| $^{294}_{117}\text{Ts}$ | 11.18 ± 0.04 | 51^{+38}_{-16} ms | 26.12 ms | 138.26 ms | 43.07 ms | 214.73 ms |
| $^{293}_{117}\text{Ts}$ | 11.32 ± 0.05 | 22^{+8}_{-4} ms | 7.37 ms | 28.43 ms | 13.52 ms | 20.12 ms |
| $^{293}_{116}\text{Lv}$ | 10.71 ± 0.02 | 57^{+43}_{-17} ms | 115.51 ms | 986.48 ms | 115.34 ms | 307.02 ms |
| $^{292}_{116}\text{Lv}$ | 10.78 ± 0.02 | 13^{+7}_{-4} ms | 50.22 ms | 55.59 ms | 27.81 ms | 56.59 ms |
| $^{291}_{116}\text{Lv}$ | 10.89 ± 0.07 | 19^{+17}_{-6} ms | 42.20 ms | 336.41 ms | 47.45 ms | 147.11 ms |
| $^{290}_{116}\text{Lv}$ | 11.00 ± 0.07 | $8.3^{+3.5}_{-1.9}$ ms | 14.72 ms | 15.17 ms | 9.52 ms | 20.74 ms |
| $^{290}_{115}\text{Mc}$ | 10.41 ± 0.04 | 650^{+490}_{-200} ms | 596.71 ms | 3426.07 ms | 733.88 ms | 4495.74 ms |
| $^{289}_{115}\text{Mc}$ | 10.49 ± 0.05 | 330^{+120}_{-80} ms | 224.91 ms | 947.54 ms | 292.70 ms | 573.54 ms |
| $^{288}_{115}\text{Mc}$ | 10.63 ± 0.01 | 164^{+30}_{-21} ms | 164.71 ms | 883.36 ms | 238.47 ms | 1577.18 ms |
| $^{287}_{115}\text{Mc}$ | 10.76 ± 0.05 | 37^{+44}_{-13} ms | 46.90 ms | 183.99 ms | 75.18 ms | 144.65 ms |
| $^{289}_{114}\text{Fl}$ | 9.98 ± 0.02 | $1.9^{+0.7}_{-0.4}$ s | 2.57 s | 23.41 s | 1.96 s | 6.09 s |
| $^{288}_{114}\text{Fl}$ | 10.07 ± 0.03 | $0.66^{+0.14}_{-0.10}$ s | 0.94 s | 1.11 s | 0.41 s | 0.96 s |
| $^{287}_{114}\text{Fl}$ | 10.17 ± 0.02 | $0.48^{+0.14}_{-0.09}$ s | 0.79 s | 6.79 s | 0.70 s | 2.56 s |
| $^{286}_{114}\text{Fl}$ | 10.35 ± 0.04 | $0.12^{+0.04}_{-0.02}$ s | 0.17 s | 0.19 s | 0.09 s | 0.22 s |
| $^{286}_{113}\text{Nh}$ | 9.79 ± 0.05 | $9.5^{+6.3}_{-2.7}$ s | 7.24 s | 43.81 s | 7.64 s | 49.12 s |
| $^{285}_{113}\text{Nh}$ | 10.01 ± 0.04 | $4.2^{+1.4}_{-0.8}$ s | 1.04 s | 4.64 s | 1.36 s | 2.43 s |
| $^{284}_{113}\text{Nh}$ | 10.12 ± 0.01 | $0.91^{+0.17}_{-0.13}$ s | 0.88 s | 5.01 s | 1.24 s | 7.83 s |
| $^{283}_{113}\text{Nh}$ | 10.38 ± 0.01 | 75^{+136}_{-30} ms | 106.87 ms | 444.13 ms | 190.80 ms | 308.77 ms |
| $^{282}_{113}\text{Nh}$ | 10.78 ± 0.08 | 73^{+134}_{-29} ms | 16.94 ms | 88.61 ms | 42.50 ms | 176.07 ms |
| $^{285}_{112}\text{Cn}$ | 9.32 ± 0.02 | 28^{+9}_{-6} s | 50.26 s | 476.82 s | 31.19 s | 104.53 s |
| $^{283}_{112}\text{Cn}$ | 9.66 ± 0.02 | $4.2^{+1.1}_{-0.7}$ s | 4.94 s | 44.20 s | 4.22 s | 14.47 s |
| $^{281}_{112}\text{Cn}$ | 10.46 ± 0.04 | $0.10^{+0.46}_{-0.05}$ s | 0.03 s | 0.26 s | 0.06 s | 0.11 s |
| $^{282}_{111}\text{Rg}$ | 9.16 ± 0.03 | 100^{+70}_{-30} s | 123.21 s | 768.17 s | 109.59 s | 739.77 s |
| $^{281}_{111}\text{Rg}$ | 9.41 ± 0.05 | 17^{+6}_{-3} s | 12.63 s | 58.35 s | 14.56 s | 26.60 s |
| $^{280}_{111}\text{Rg}$ | 9.91 ± 0.01 | $4.6^{+0.8}_{-0.7}$ s | 0.74 s | 4.39 s | 1.40 s | 6.02 s |
| $^{279}_{111}\text{Rg}$ | 10.53 ± 0.16 | 90^{+170}_{-40} ms | 9.94 ms | 42.67 ms | 32.67 ms | 26.66 ms |
| $^{278}_{111}\text{Rg}$ | 10.85 ± 0.08 | $4.2^{+7.5}_{-1.7}$ ms | 2.72 ms | 14.68 ms | 11.31 ms | 26.64 ms |
| $^{281}_{110}\text{Ds}$ | 8.85 ± 0.03 | $12.7^{+4.0}_{-2.5}$ s | 320.73 s | 3093.88 s | 199.99 s | 572.52 s |
| $^{279}_{110}\text{Ds}$ | 9.85 ± 0.02 | $0.21^{+0.04}_{-0.04}$ s | 0.29 s | 2.74 s | 0.51 s | 0.78 s |
| $^{277}_{110}\text{Ds}$ | 10.72 ± 0.04 | $0.006^{+0.027}_{-0.003}$ s | 0.002 s | 0.01 s | 0.005 s | 0.006 s |
| $^{278}_{109}\text{Ms}$ | 9.58 ± 0.03 | $4.5^{+3.5}_{-1.3}$ s | 1.29 s | 8.47 s | 3.11 s | 7.08 s |
| $^{276}_{109}\text{Ms}$ | 10.03 ± 0.01 | $0.45^{+0.12}_{-0.09}$ s | 0.08 s | 0.46 s | 0.26 s | 0.56 s |
| $^{275}_{109}\text{Ms}$ | 10.48 ± 0.01 | 20^{+24}_{-7} ms | 3.09 ms | 13.72 ms | 15.30 ms | 7.78 ms |
| $^{274}_{109}\text{Ms}$ | 10.2 ± 1.1 | 440^{+810}_{-170} ms | 28.05 ms | 160.76 ms | 105.82 ms | 258.18 ms |
| $^{275}_{108}\text{Hs}$ | 9.45 ± 0.02 | $0.20^{+0.18}_{-0.06}$ s | 0.87 s | 8.39 s | 1.71 s | 2.09 s |

Since each clusterization state describes the same nucleus, all these states should share the same eigenenergy, which is equal to the total energy E of the total wave function. Thus we have

$$E = \sum_i^{N_s} |a_i|^2 E = \sum_i E_{fi}, \quad (17)$$

where E_{fi} is the formation energy for a cluster in the clusterization state (i) and it is responsible for the formation of the cluster and represents the intrinsic energy of the cluster. In the CFM, values of both the formation energy and the total energy of the considered system are extracted from the experimental binding energy. The preformation factor, S_{α} , can be evaluated

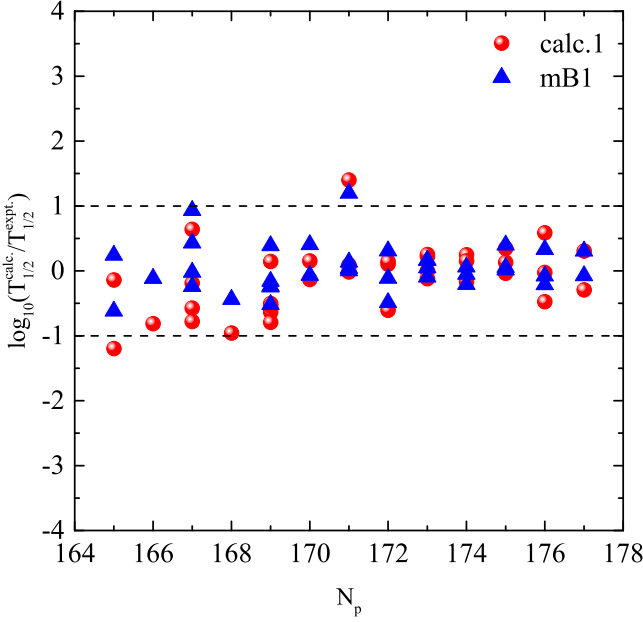


FIG. 1. Deviation of the calculated α -decay half-lives, $T_{1/2}^{\text{calc.1}}$ and $T_{1/2}^{\text{mB1}}$, with the corresponding experimental data for the recently synthesized SHN listed in Table I.

by

$$S_\alpha = \frac{E_{f\alpha}}{E}, \quad (18)$$

where $E_{f\alpha}$ is the formation energy of the α cluster, and E is actually composed of the formation energy (intrinsic energy) of the α cluster and the interaction energy between the α cluster and residual nucleons.

A comprehensive formula of the formation energy for even-even, odd- A , and odd-odd nuclei can be written in terms of the separation energies as [62,63]

$$E_{f\alpha} = \begin{cases} 2S_p + 2S_n - S_c & \text{(even-even),} \\ 2S_p + S_{2n} - S_c & \text{(even-odd),} \\ S_{2p} + 2S_n - S_c & \text{(odd-even),} \\ S_{2p} + S_{2n} - S_c & \text{(odd-odd),} \end{cases} \quad (19)$$

$$E = S_c(A, Z), \quad (20)$$

where S_{2p} (S_{2n}) is the two-proton (neutron) separation energy defined in terms of the binding energies as [63]

$$S_{2p}(A, Z) = B(A, Z) - B(A - 2, Z - 2), \quad (21)$$

$$S_{2n}(A, Z) = B(A, Z) - B(A - 2, Z). \quad (22)$$

The α -cluster separation energy S_c is defined as

$$S_c(A, Z) = B(A, Z) - B(A - 4, Z - 2), \quad (23)$$

where $B(A, Z)$ is the binding energy of a nucleus of mass number A and atomic number Z . Beside the above described method of calculating $T_{1/2}$ for α -decay of SHN, we consider three other semiempirical formulas. These formulas together with the microscopic double folding model succeeded in reproducing α -decay half-lives for a large number of heavy and

superheavy nuclei. We now consider briefly the three empirical formulas for calculating α -decay half-lives.

A. The Viola-Seaborg semiempirical formula (VSS)

The phenomenological formula of Viola and Seaborg, with constants determined by Sobiczewski *et al.* [47], is given by

$$\log_{10}(T_{1/2}^{\text{VSS}}) = (aZ + b)Q^{-1/2} + cZ + d + h_{\log}. \quad (24)$$

Here the half-life $T_{1/2}$ is in seconds, the Q value is in MeV, and Z is the atomic number of the parent nucleus. The quantities a , b , c , and d are adjustable parameters obtained through a least-squares fit to even-even nuclei and the quantity h_{\log} represents the hindrance factor for nuclei with unpaired nucleons.

Instead of using the original set of constants given by Viola and Seaborg [46], Sobiczewski *et al.* [47] readjusted them to better reproduce the experimental data (especially for the heaviest nuclides) by taking into account new data for even-even nuclei. The constants are $a = 1.66175$, $b = -8.5166$, $c = -0.20228$, $d = -33.9069$, and

$$h_{\log} = \begin{cases} 0 & \text{for } Z, N \text{ even,} \\ 0.772 & \text{for } Z \text{ odd, } N \text{ even,} \\ 1.066 & \text{for } Z \text{ even, } N \text{ odd,} \\ 1.114 & \text{for } Z, N \text{ odd.} \end{cases}$$

B. Modified Brown formula (mB1)

We will adopt in the present work the modified Brown (mB1) formula with an additional hindrance term depending on parity [51]:

$$\log_{10}(T_{1/2}^{\text{mB1}}) = a(Z - 2)^b Q^{-1/2} + c + h^{\text{mB1}}. \quad (25)$$

The constants are $a = 13.0705$, $b = 0.5182$, $c = -47.8867$, and

$$h^{\text{mB1}} = \begin{cases} 0 & \text{for } Z, N \text{ even,} \\ 0.6001 & \text{for } Z \text{ odd, } N \text{ even,} \\ 0.4666 & \text{for } Z \text{ even, } N \text{ odd,} \\ 0.8200 & \text{for } Z, N \text{ odd.} \end{cases}$$

C. Semiempirical formula based on fission theory (SemFIS2)

Poenaru *et al.* [53] proposed semiempirical formula for α -decay half-lives based on fission theory (SemFIS2) which is expressed as

$$\log_{10}(T_{1/2}^{\text{SemFIS2}}) = 0.43429 \chi(x, y) K - 20.446 + H^f, \quad (26)$$

where

$$K = 2.52956 Z_d [A_d / (A Q)]^{1/2} [\arccos \sqrt{r} - \sqrt{r(1-r)}], \quad (27)$$

and $r = 0.423 Q(1.5874 + A_d^{1/3}) / Z_d$. The numerical coefficient χ , close to unity, is a second-order polynomial:

$$\chi(x, y) = B_1 + x(B_2 + x B_4) + y(B_3 + y B_6) + x y B_5. \quad (28)$$

TABLE II. Predicted α -decay half-lives using the double-folding model with constant preformation factor, $T_{1/2}^{\text{calc1}}$; the double-folding model with preformation factor extracted from cluster formation model, $T_{1/2}^{\text{calc2}}$; the Viola-Seaborg-Sobiczewski (VSS) formula [46,47], $T_{1/2}^{\text{VSS}}$; the modified Brown (mB1) formula [51], $T_{1/2}^{\text{mB1}}$; and the semiempirical formula [53], $T_{1/2}^{\text{SemFIS2}}$. The extracted preformation probabilities, S_α , from the cluster formation model (CFM) are also listed. The Q values are extracted from the recent WS4+ mass model [55] (often denoted as WS4 + RBF) are Weizsacker-Skyrme models applying the radial basis function (RBF) approach.

| Parent nuclei | $Q_\alpha^{\text{WS4+}}$ (MeV) | S_α | $T_{1/2}^{\text{calc1}}$ (s) | $T_{1/2}^{\text{calc2}}$ (s) | $T_{1/2}^{\text{VSS}}$ (s) | $T_{1/2}^{\text{mB1}}$ (s) | $T_{1/2}^{\text{SemFIS2}}$ (s) | T_{SF} (s) |
|----------------------------------|--------------------------------|------------|------------------------------|------------------------------|----------------------------|----------------------------|--------------------------------|-----------------------|
| ²⁹⁰ ₁₁₈ Og | 12.572 | 0.239 | 1.75×10^{-5} | 2.85×10^{-5} | 1.33×10^{-5} | 2.53×10^{-5} | 2.95×10^{-5} | 1.79×10^{10} |
| ²⁸⁶ ₁₁₆ Lv | 11.280 | 0.218 | 3.43×10^{-3} | 6.12×10^{-3} | 3.07×10^{-3} | 2.55×10^{-3} | 5.83×10^{-3} | 4.26×10^5 |
| ²⁸² ₁₁₄ Fl | 11.340 | 0.264 | 6.17×10^{-4} | 9.12×10^{-4} | 5.75×10^{-4} | 7.47×10^{-4} | 1.00×10^{-3} | 1.79×10^2 |
| ²⁷⁸ ₁₁₂ Cn | 11.739 | 0.253 | 2.01×10^{-5} | 3.10×10^{-5} | 1.88×10^{-5} | 4.98×10^{-5} | 3.15×10^{-5} | 1.10×10^0 |
| ²⁷⁴ ₁₁₀ Ds | 10.896 | 0.222 | 4.24×10^{-4} | 7.45×10^{-4} | 4.35×10^{-4} | 8.39×10^{-4} | 6.39×10^{-4} | 8.02×10^{-2} |
| ²⁷⁰ ₁₀₈ Hs | 9.135 | 0.214 | 5.89×10^0 | 1.08×10^1 | 6.43×10^0 | 3.81×10^0 | 8.59×10^0 | 5.78×10^{-2} |
| ²⁶⁶ ₁₀₆ Sg | 8.566 | 0.206 | 7.71×10^1 | 1.46×10^2 | 8.43×10^1 | 4.71×10^1 | 1.06×10^2 | 3.40×10^{-1} |
| ²⁶² ₁₀₄ Rf | 8.431 | 0.204 | 3.95×10^1 | 7.56×10^1 | 4.39×10^1 | 3.70×10^1 | 5.00×10^1 | 1.36×10^1 |
| ²⁹¹ ₁₁₈ Og | 12.391 | 0.120 | 6.28×10^{-5} | 1.31×10^{-4} | 3.76×10^{-4} | 1.53×10^{-4} | 2.89×10^{-4} | 1.20×10^{10} |
| ²⁸⁷ ₁₁₆ Lv | 11.252 | 0.103 | 6.05×10^{-3} | 1.47×10^{-2} | 4.18×10^{-2} | 8.49×10^{-3} | 2.77×10^{-2} | 2.76×10^5 |
| ²⁸³ ₁₁₄ Fl | 10.843 | 0.152 | 1.49×10^{-2} | 2.46×10^{-2} | 1.10×10^{-1} | 2.26×10^{-2} | 6.56×10^{-2} | 1.13×10^2 |
| ²⁷⁹ ₁₁₂ Cn | 11.384 | 0.130 | 1.87×10^{-4} | 3.59×10^{-4} | 1.38×10^{-3} | 6.89×10^{-4} | 7.74×10^{-4} | 6.68×10^{-1} |
| ²⁷⁵ ₁₁₀ Ds | 10.933 | 0.115 | 5.23×10^{-4} | 1.14×10^{-3} | 4.12×10^{-3} | 2.06×10^{-3} | 2.07×10^{-3} | 4.73×10^{-2} |
| ²⁷¹ ₁₀₈ Hs | 9.346 | 0.112 | 2.02×10^0 | 4.49×10^0 | 1.71×10^1 | 3.14×10^0 | 7.56×10^0 | 3.30×10^{-2} |
| ²⁶⁷ ₁₀₆ Sg | 8.274 | 0.101 | 1.20×10^3 | 2.97×10^3 | 9.85×10^3 | 1.02×10^3 | 4.21×10^3 | 1.88×10^{-1} |
| ²⁶³ ₁₀₄ Rf | 8.122 | 0.103 | 7.16×10^2 | 1.74×10^3 | 5.95×10^3 | 9.26×10^2 | 2.28×10^3 | 7.26×10^0 |
| ²⁹² ₁₁₈ Og | 12.212 | 0.235 | 9.40×10^{-5} | 1.56×10^{-4} | 7.92×10^{-5} | 1.09×10^{-4} | 1.54×10^{-4} | 5.32×10^9 |
| ²⁸⁸ ₁₁₆ Lv | 11.259 | 0.206 | 3.62×10^{-3} | 6.86×10^{-3} | 3.45×10^{-3} | 2.81×10^{-3} | 5.81×10^{-3} | 1.19×10^5 |
| ²⁸⁴ ₁₁₄ Fl | 10.539 | 0.246 | 5.61×10^{-2} | 8.88×10^{-2} | 5.80×10^{-2} | 3.49×10^{-2} | 8.69×10^{-2} | 4.70×10^1 |
| ²⁸⁰ ₁₁₂ Cn | 10.830 | 0.251 | 2.39×10^{-3} | 3.71×10^{-3} | 2.54×10^{-3} | 3.09×10^{-3} | 3.44×10^{-3} | 2.69×10^{-1} |
| ²⁷⁶ ₁₁₀ Ds | 10.872 | 0.220 | 4.55×10^{-4} | 8.06×10^{-4} | 4.98×10^{-4} | 9.40×10^{-4} | 6.20×10^{-4} | 1.85×10^{-2} |
| ²⁷² ₁₀₈ Hs | 9.582 | 0.206 | 2.54×10^{-1} | 4.81×10^{-1} | 2.97×10^{-1} | 2.73×10^{-1} | 3.21×10^{-1} | 1.25×10^{-2} |
| ²⁶⁸ ₁₀₆ Sg | 8.093 | 0.187 | 3.38×10^3 | 7.06×10^3 | 3.76×10^3 | 1.26×10^3 | 3.93×10^3 | 6.88×10^{-2} |
| ²⁶⁴ ₁₀₄ Rf | 7.868 | 0.195 | 3.83×10^3 | 7.68×10^3 | 4.29×10^3 | 2.03×10^3 | 3.99×10^3 | 2.57×10^0 |
| ²⁹³ ₁₁₈ Og | 12.214 | 0.121 | 1.41×10^{-4} | 2.91×10^{-4} | 9.13×10^{-4} | 3.16×10^{-4} | 6.02×10^{-4} | 1.56×10^9 |
| ²⁸⁹ ₁₁₆ Lv | 11.146 | 0.098 | 1.03×10^{-2} | 2.63×10^{-2} | 7.62×10^{-2} | 1.39×10^{-2} | 4.28×10^{-2} | 3.38×10^4 |
| ²⁸⁵ ₁₁₄ Fl | 10.249 | 0.124 | 5.11×10^{-1} | 1.03×10^0 | 4.10×10^0 | 4.59×10^{-1} | 2.04×10^0 | 1.30×10^1 |
| ²⁸¹ ₁₁₂ Cn | 10.455 | 0.122 | 3.23×10^{-2} | 6.64×10^{-2} | 2.69×10^{-1} | 5.79×10^{-2} | 1.18×10^{-1} | 7.20×10^{-2} |
| ²⁷⁷ ₁₁₀ Ds | 10.547 | 0.113 | 4.34×10^{-3} | 9.64×10^{-3} | 3.724×10^{-2} | 1.336×10^{-2} | 1.49×10^{-2} | 4.78×10^{-3} |
| ²⁷³ ₁₀₈ Hs | 9.611 | 0.108 | 3.164×10^{-1} | 7.35×10^{-1} | 2.86×10^0 | 6.79×10^{-1} | 9.92×10^{-1} | 3.13×10^{-3} |
| ²⁶⁹ ₁₀₆ Sg | 8.338 | 0.098 | 6.683×10^2 | 1.70×10^3 | 5.88×10^3 | 6.50×10^2 | 1.87×10^3 | 1.67×10^{-2} |
| ²⁶⁵ ₁₀₄ Rf | 7.550 | 0.098 | 1.01×10^5 | 2.57×10^5 | 8.30×10^5 | 6.93×10^4 | 2.48×10^5 | 6.05×10^{-1} |
| ²⁹⁴ ₁₁₈ Og | 12.171 | 0.219 | 1.08×10^{-4} | 1.93×10^{-4} | 9.75×10^{-5} | 1.29×10^{-4} | 1.59×10^{-4} | 3.05×10^8 |
| ²⁹⁰ ₁₁₆ Lv | 11.056 | 0.202 | 1.07×10^{-2} | 2.06×10^{-2} | 1.10×10^{-2} | 7.28×10^{-3} | 1.50×10^{-2} | 6.39×10^3 |
| ²⁸⁶ ₁₁₄ Fl | 9.940 | 0.205 | 2.36×10^0 | 4.48×10^0 | 2.62×10^0 | 8.35×10^{-1} | 3.16×10^0 | 2.37×10^0 |
| ²⁸² ₁₁₂ Cn | 10.112 | 0.200 | 1.67×10^{-1} | 3.26×10^{-1} | 1.94×10^{-1} | 1.18×10^{-1} | 2.03×10^{-1} | 1.28×10^{-2} |
| ²⁷⁸ ₁₁₀ Ds | 10.231 | 0.212 | 1.77×10^{-2} | 3.26×10^{-2} | 2.13×10^{-2} | 2.28×10^{-2} | 1.98×10^{-2} | 8.21×10^{-4} |
| ²⁷⁴ ₁₀₈ Hs | 9.521 | 0.196 | 3.58×10^{-1} | 7.12×10^{-1} | 4.47×10^{-1} | 3.87×10^{-1} | 3.62×10^{-1} | 5.20×10^{-4} |
| ²⁷⁰ ₁₀₆ Sg | 8.634 | 0.187 | 4.02×10^1 | 8.40×10^1 | 5.01×10^1 | 3.00×10^1 | 3.58×10^1 | 2.69×10^{-3} |
| ²⁶⁶ ₁₀₄ Rf | 7.327 | 0.181 | 5.21×10^5 | 1.12×10^6 | 5.70×10^5 | 1.46×10^5 | 3.89×10^5 | 9.44×10^{-2} |

TABLE II. (Continued.)

| Parent nuclei | $Q_\alpha^{\text{WS4+}}$ (MeV) | S_α | $T_{1/2}^{\text{calc1}}$ (s) | $T_{1/2}^{\text{calc2}}$ (s) | $T_{1/2}^{\text{VSS}}$ (s) | $T_{1/2}^{\text{mb1}}$ (s) | $T_{1/2}^{\text{SemFIS2}}$ (s) | T_{SF} (s) |
|-------------------------|--------------------------------|------------|------------------------------|------------------------------|----------------------------|----------------------------|--------------------------------|-----------------------|
| $^{295}_{118}\text{Og}$ | 11.876 | 0.101 | 7.37×10^{-4} | 1.83×10^{-3} | 5.23×10^{-3} | 1.32×10^{-3} | 2.72×10^{-3} | 3.94×10^7 |
| $^{291}_{116}\text{Lv}$ | 11.093 | 0.092 | 1.31×10^{-2} | 3.55×10^{-2} | 4.05×10^{-1} | 4.63×10^{-2} | 2.99×10^{-1} | 8.00×10^2 |
| $^{287}_{114}\text{Fl}$ | 9.742 | 0.100 | 1.36×10^1 | 3.39×10^1 | 1.16×10^2 | 7.44×10^0 | 4.43×10^1 | 2.88×10^{-1} |
| $^{283}_{112}\text{Cn}$ | 9.816 | 0.107 | 1.73×10^0 | 4.036×10^0 | 1.55×10^1 | 1.75×10^0 | 5.06×10^0 | 1.50×10^{-3} |
| $^{279}_{110}\text{Ds}$ | 9.838 | 0.129 | 3.18×10^{-1} | 6.15×10^{-1} | 2.96×10^0 | 5.47×10^{-1} | 8.46×10^{-1} | 9.35×10^{-5} |
| $^{275}_{108}\text{Hs}$ | 9.264 | 0.093 | 3.15×10^0 | 8.46×10^0 | 3.01×10^1 | 5.12×10^0 | 7.45×10^0 | 5.74×10^{-5} |
| $^{271}_{106}\text{Sg}$ | 8.617 | 0.092 | 6.93×10^1 | 1.88×10^2 | 6.64×10^2 | 9.84×10^1 | 1.42×10^2 | 2.87×10^{-4} |
| $^{267}_{104}\text{Rf}$ | 7.548 | 0.094 | 9.65×10^4 | 2.58×10^5 | 8.45×10^5 | 7.04×10^4 | 1.62×10^5 | 9.76×10^{-3} |
| $^{296}_{118}\text{Og}$ | 11.726 | 0.199 | 1.01×10^{-3} | 1.97×10^{-3} | 1.00×10^{-3} | 8.67×10^{-4} | 1.22×10^{-3} | 3.37×10^6 |
| $^{292}_{116}\text{Lv}$ | 11.100 | 0.191 | 7.81×10^{-3} | 1.60×10^{-2} | 8.52×10^{-3} | 5.91×10^{-3} | 8.79×10^{-3} | 6.65×10^1 |
| $^{288}_{114}\text{Fl}$ | 9.618 | 0.197 | 1.99×10^1 | 3.94×10^1 | 2.35×10^1 | 5.19×10^0 | 2.05×10^1 | 2.32×10^{-2} |
| $^{284}_{112}\text{Cn}$ | 9.518 | 0.209 | 8.18×10^0 | 1.52×10^1 | 1.01×10^1 | 3.28×10^0 | 7.49×10^0 | 1.17×10^{-4} |
| $^{280}_{110}\text{Ds}$ | 9.415 | 0.226 | 3.40×10^0 | 5.87×10^0 | 4.36×10^0 | 2.09×10^0 | 2.77×10^0 | 7.06×10^{-6} |
| $^{276}_{108}\text{Hs}$ | 9.057 | 0.190 | 8.56×10^0 | 1.75×10^1 | 1.13×10^1 | 6.15×10^0 | 6.15×10^0 | 4.20×10^{-6} |
| $^{272}_{106}\text{Sg}$ | 8.460 | 0.186 | 1.47×10^2 | 3.08×10^2 | 1.92×10^2 | 9.61×10^1 | 8.96×10^1 | 2.03×10^{-5} |
| $^{268}_{104}\text{Rf}$ | 7.792 | 0.179 | 6.58×10^3 | 1.43×10^4 | 8.26×10^3 | 3.60×10^3 | 3.30×10^3 | 6.69×10^{-4} |
| $^{297}_{118}\text{Og}$ | 12.078 | 0.101 | 2.47×10^{-4} | 6.10×10^{-4} | 1.83×10^{-3} | 5.58×10^{-4} | 7.26×10^{-4} | 1.92×10^5 |
| $^{293}_{116}\text{Lv}$ | 10.767 | 0.099 | 8.21×10^{-2} | 2.08×10^{-1} | 7.00×10^{-1} | 8.69×10^{-2} | 2.18×10^{-1} | 3.66×10^0 |
| $^{289}_{114}\text{Fl}$ | 9.579 | 0.104 | 3.97×10^1 | 9.56×10^1 | 3.60×10^2 | 1.91×10^1 | 9.35×10^1 | 1.24×10^{-3} |
| $^{285}_{112}\text{Cn}$ | 9.207 | 0.101 | 1.15×10^2 | 2.86×10^2 | 1.08×10^3 | 6.21×10^1 | 2.37×10^2 | 6.05×10^{-6} |
| $^{281}_{110}\text{Ds}$ | 8.960 | 0.111 | 1.39×10^2 | 3.12×10^2 | 1.35×10^3 | 9.88×10^1 | 2.49×10^2 | 3.53×10^{-7} |
| $^{277}_{108}\text{Hs}$ | 8.950 | 0.093 | 2.84×10^1 | 7.59×10^1 | 2.86×10^2 | 3.51×10^1 | 4.51×10^1 | 2.03×10^{-7} |
| $^{273}_{106}\text{Sg}$ | 8.232 | 0.093 | 1.40×10^3 | 3.77×10^3 | 1.39×10^4 | 1.37×10^3 | 1.83×10^3 | 9.55×10^{-7} |
| $^{269}_{104}\text{Rf}$ | 7.700 | 0.089 | 2.26×10^4 | 6.37×10^4 | 2.16×10^5 | 2.13×10^4 | 2.38×10^4 | 3.04×10^{-5} |
| $^{298}_{118}\text{Og}$ | 12.158 | 0.219 | 1.03×10^{-4} | 1.83×10^{-4} | 1.04×10^{-4} | 1.36×10^{-4} | 9.65×10^{-5} | 7.22×10^3 |
| $^{294}_{116}\text{Lv}$ | 10.639 | 0.187 | 1.10×10^{-1} | 2.30×10^{-1} | 1.31×10^{-1} | 5.63×10^{-2} | 9.03×10^{-2} | 1.34×10^{-1} |
| $^{290}_{114}\text{Fl}$ | 9.495 | 0.203 | 4.47×10^1 | 8.61×10^1 | 5.59×10^1 | 1.07×10^1 | 3.15×10^1 | 4.37×10^{-5} |
| $^{286}_{112}\text{Cn}$ | 9.014 | 0.185 | 3.03×10^2 | 6.41×10^2 | 3.90×10^2 | 7.09×10^1 | 1.83×10^2 | 2.07×10^{-7} |
| $^{282}_{110}\text{Ds}$ | 8.515 | 0.194 | 2.83×10^3 | 5.70×10^3 | 3.68×10^3 | 6.35×10^2 | 1.43×10^3 | 1.17×10^{-8} |
| $^{278}_{108}\text{Hs}$ | 8.760 | 0.192 | 7.36×10^1 | 1.50×10^2 | 1.01×10^2 | 4.05×10^1 | 3.32×10^1 | 6.54×10^{-9} |
| $^{274}_{106}\text{Sg}$ | 8.051 | 0.185 | 4.00×10^3 | 8.42×10^3 | 5.36×10^3 | 1.71×10^3 | 1.43×10^3 | 2.97×10^{-8} |
| $^{270}_{104}\text{Rf}$ | 7.477 | 0.175 | 1.09×10^5 | 2.44×10^5 | 1.39×10^5 | 4.25×10^4 | 3.05×10^4 | 9.17×10^{-7} |

In Ref. [53], the following set of parameter values is obtained for transuranium nuclei: $B_1 = 0.985415$, $B_2 = 0.102199$, $B_3 = -0.024863$, $B_4 = -0.832081$, $B_5 = 1.50572$, and $B_6 = -0.681221$. The hindrance factor H^f takes different values: $H_{ee}^f = 0$ for even-even emitters, $H_{eo}^f = 0.63$, $H_{oe}^f = 0.51$, and $H_{oo}^f = 1.26$. The reduced variables x and y are defined as

$$x \equiv (N - N_i)/(N_{i+1} - N_i), \quad N_i < N \leq N_{i+1}, \quad (29)$$

$$y \equiv (Z - Z_i)/(Z_{i+1} - Z_i), \quad Z_i < Z \leq Z_{i+1}, \quad (30)$$

with $N_i = \dots, 51, 83, 127, 185, 229, \dots$, $Z_i = \dots, 29, 51, 83, 127, \dots$; hence for the region of superheavy nuclei $x = (N - 127)/(185 - 127)$, $y = (Z - 83)/(127 - 83)$.

D. Spontaneous fission half-lives

To identify the mode of decay of Og isotopes, the spontaneous-fission half-lives were evaluated using the semiempirical formula given by Xu *et al.* [78]:

$$T_{1/2} = \exp \left\{ 2\pi \left[C_0 + C_1 A + C_2 Z^2 + C_3 Z^4 + C_4 (N - Z)^2 - \left(0.13323 \frac{Z^2}{A^{1/3}} - 11.64 \right) \right] \right\}. \quad (31)$$

The constants are $C_0 = -195.09227$, $C_1 = 3.10156$, $C_2 = -0.04386$, $C_3 = 1.4030 \times 10^{-6}$, and $C_4 = -0.03199$.

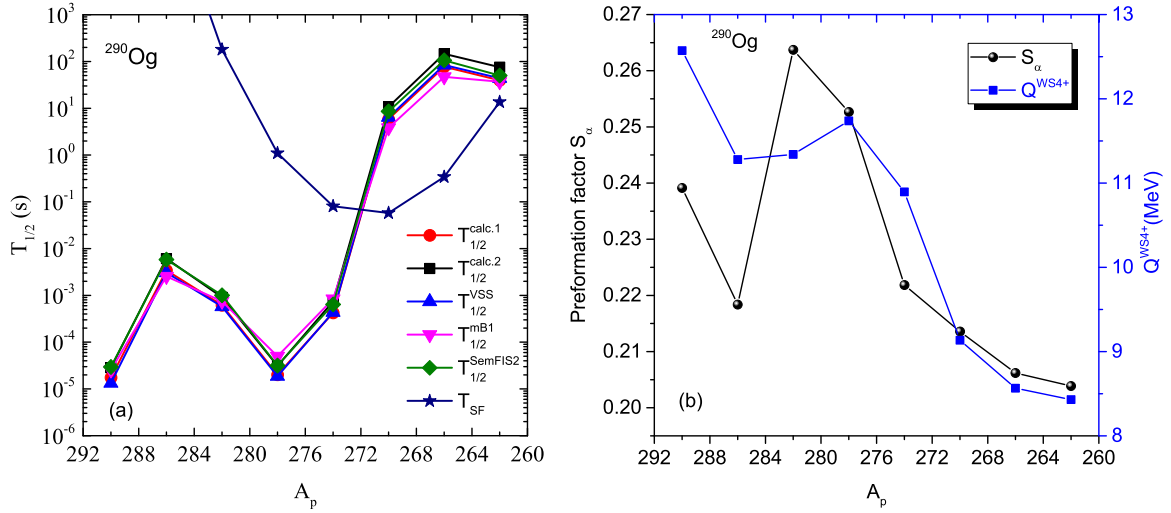


FIG. 2. (a) Comparison of the calculated α -decay half-lives of the isotope $^{290}_{118}\text{Og}$ and products on its α -decay chain. (b) Variation of the α -preformation factor and the Q value extracted from the recent WS4+ mass model of the isotope $^{290}_{118}\text{Og}$ and its corresponding α -decay chain versus parent mass number A_p .

III. RESULTS AND DISCUSSION

We have investigated the α -decay half-lives of recently synthesized superheavy nuclei by employing the density dependent cluster model. The recent experimental values of the (Q_α) are used [37]. The double-folding model is employed to establish the α -nucleus potential using a realistic effective M3Y-Paris NN interaction [69,76,77] with finite-range exchange force. The main effect of antisymmetrization under exchange of nucleons between the α and the daughter nuclei has been included in the folding model through the finite-range exchange part of the NN interaction. The penetration probability is obtained from the WKB approximation in combination with the Bohr-Sommerfeld quantization condition. The results obtained for α -decay half-lives ($T_{1/2}^{\text{calc.1}}$) of recently synthesized superheavy nuclei are compared with the available experimental results [37]. In the calculations of $T_{1/2}^{\text{calc.1}}$, we take the same preformation factor S_α for a certain kind of nuclei (even-even, odd- A , and odd-odd). The motivation for this is clearly shown in Ref. [61]. In the present study, we use the preformation factor $S_\alpha = 0.39$ for even-even nuclei, $S_\alpha = 0.25$ for odd- A nuclei and $S_\alpha = 0.15$ for odd-odd nuclei, as described in Ref. [61]. It is seen that the theoretical predictions are in good agreement with the experimental observations. For theoretical comparison, the results of α -decay half-lives are calculated with the Viola-Seaborg-Sobiczewski (VSS) formula [46,47], the modified Brown (mB1) formula [51], and the semiempirical formula based on fission theory (SemFIS2) [53] using the same experimental Q_α values [37], and are shown in Table I.

To show the effective strength of our calculations, we have evaluated the standard deviation, σ , for the logarithmic half-lives between the experimental and calculated values using the following equation:

$$\sigma = \left[\frac{1}{n-1} \sum_{i=1}^n (\log_{10} T_{1/2}^{\text{calc.}} - \log_{10} T_{1/2}^{\text{expt.}})^2 \right]^{1/2}. \quad (32)$$

The standard deviation of the logarithmic half-life is found to be 0.514 for the calculations of $T_{1/2}^{\text{calc.1}}$, 0.826 for the Viola-Seaborg-Sobiczewski (VSS) formula, 0.366 for the modified Brown (mB1) formula, and 0.625 for the semiempirical formula based on fission theory (SemFIS2).

Figure 1 displays the deviations of calculated α -decay half-lives $T_{1/2}^{\text{calc.1}}$ and $T_{1/2}^{\text{mB1}}$ from the experimental data as a function of the neutron number N of the parent nucleus for the recently synthesized SHN listed in Table I. It is clear from Fig. 1 that the deviations of calculated α -decay half-lives with the corresponding experimental data lie within the order 1 and most of the points lie near $\log_{10}(T_{1/2}^{\text{calc.}}/T_{1/2}^{\text{expt.}}) = 0$; this becomes

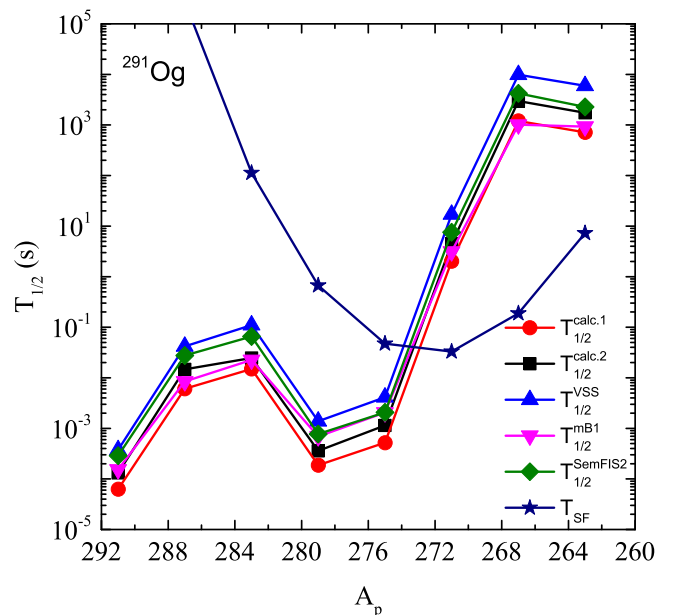


FIG. 3. The same as Fig. 2(a) but for the isotopes $^{291}_{118}\text{Og}$ and products on its α -decay chain.

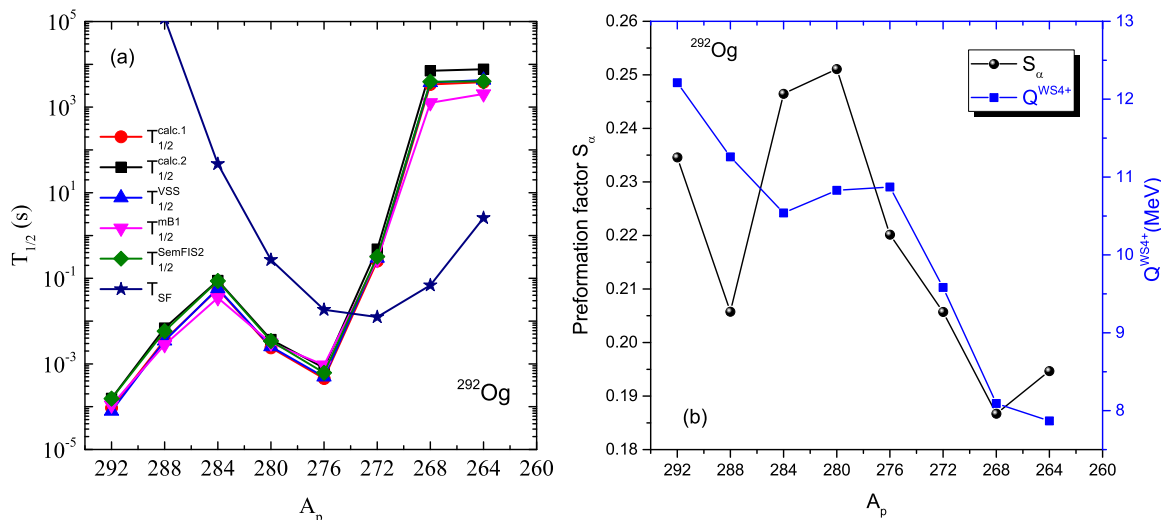


FIG. 4. The same as Fig. 2 but for the isotopes $^{292}_{118}\text{Og}$ and products on its α -decay chain.

clear as the value of the neutron number N_p becomes larger. This means that most of the calculated α -decay half-lives are in good agreement with the experimental data for the recently synthesized SHN in Table I and we can extend our calculations to the unknown isotopes of the superheavy element Og.

The α -decay half-lives of nine isotopes of the superheavy element oganesson (Og) with $Z = 118$ and their corresponding decay products are calculated. The Q_α is extracted from the WS4 mass table together with the radial basis function corrections [55]. This model is one of the most reliable mass models for the study of SHN which has an accuracy smaller than 300 keV for Q_α of SHN [55]. Two different methods are adopted for calculating the preformation probability (S_α). The first one, used in Table I, simply uses a constant value of S_α for a certain kind of nuclei, which is frequently used in previous studies [45,61]. The other method is based on the recently proposed cluster formation model (CFM) which gives realistic α preformation factors [57,62–64]. The successful determination of the preformation factor through the CFM motivates us to determine the α -decay half-lives of Og isotopes and its decay products. The formation energies of the alpha cluster were determined from the differences of the binding energies that determined from the WS4 mass model with the radial basis function corrections [55].

Table II shows the calculated α -decay half-lives for nine isotopes of element Og ($^{290-298}_{118}\text{Og}$) and their corresponding decay products using the Q_α values extracted from the recent WS4+ mass model [55]. The α -decay half-lives were calculated using five different methods: the double folding model with constant preformation factor, $T_{1/2}^{\text{calc}1}$; the double folding model with preformation factor extracted from the cluster formation model (CFM), $T_{1/2}^{\text{calc}2}$; the Viola-Seaborg-Sobiczewski formula, $T_{1/2}^{\text{VSS}}$; the modified Brown formula, $T_{1/2}^{\text{mB1}}$; and the semiempirical formula based on fission theory, $T_{1/2}^{\text{SemFIS2}}$. The values of the preformation factor, S_α , extracted from the CFM are presented on Table II. The last column of Table II presents the spontaneous fission half-lives, T_{SF} , calculated from Eq. (31).

Figures 2(a)–10(a) show comparison of the calculated α -decay half-lives, using the Q_α values extracted from the recent WS4+ mass model [55], with the spontaneous fission half-lives for the isotopes $^{290-298}_{118}\text{Og}$ and their decay products. Figure 2(a) represents the α -decay and the spontaneous fission half-lives for the element $^{290}_{118}\text{Og}$ and its α -decay chain. In Fig. 2(a), it is shown that the nuclei $^{290}_{118}\text{Og}$, $^{286}_{116}\text{Lv}$, $^{282}_{114}\text{Fl}$, $^{278}_{112}\text{Cn}$, and $^{274}_{110}\text{Ds}$ have α -decay half-lives shorter than the corresponding spontaneous fission half-lives. This means that the nucleus $^{290}_{118}\text{Og}$ survive fission and our study predicts 5α chains from the isotope $^{290}_{118}\text{Og}$. The five curves representing α decay in Fig. 2(a) are similar in behavior, and the values of $T_{1/2}$ derived from the different five methods (Table II) have the same order of magnitude. The values of $T_{1/2}$ for α decay

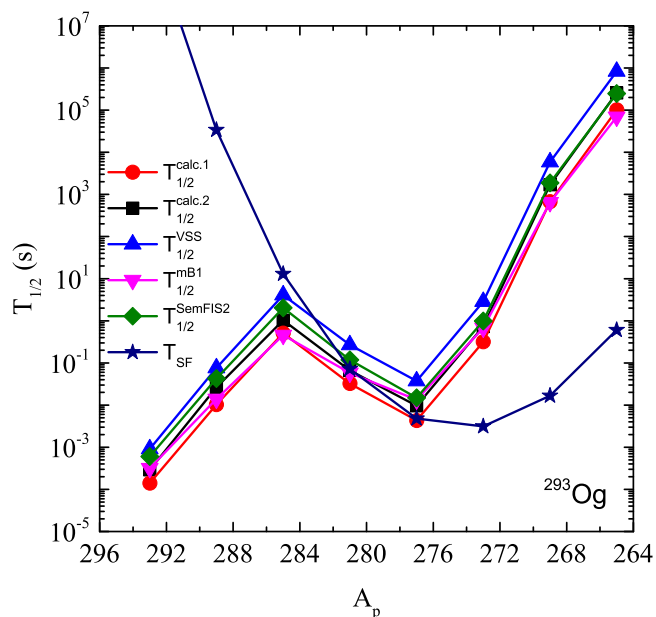


FIG. 5. The same as Fig. 2(a) but for the isotopes $^{293}_{118}\text{Og}$ and products on its α -decay chain.

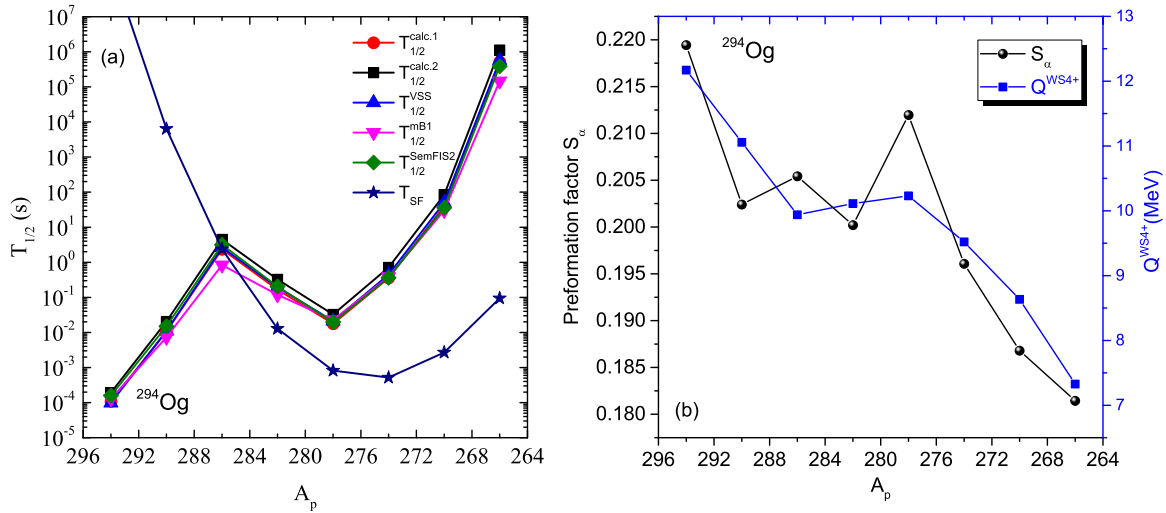


FIG. 6. The same as Fig. 2 but for the isotopes $^{294}_{118}\text{Og}$ and products on its α -decay chain.

extend from about 10^{-5} s for $^{290}_{118}\text{Og}$ to about 100 s for ^{262}Rf . The α -decay half-life time increases as the mass number A_p of the parent nucleus increases, reaches a maximum value at $A_p = 286$ and $Z_p = 116$, then decreases to a minimum value at $A_p = 278$ and $Z_p = 112$, then it increases sharply reaching $A_p = 270$ and $Z_p = 108$.

Figure 3 is the same as Fig. 2(a) but it is for the odd-mass number isotope $^{291}_{118}\text{Og}$. The element $^{291}_{118}\text{Og}$ survives fission, and the present study predicts 5α chains from the isotope $^{291}_{118}\text{Og}$. The curves representing $T_{1/2}$ of α decay have a maximum value at $A_p = 283$ and $Z_p = 114$ and a minimum value at $A_p = 279$ and $Z_p = 112$. The values of $T_{1/2}$ for α decay extend from about 10^{-4} s for $^{291}_{118}\text{Og}$ to more than 1000 s for ^{263}Rf .

Figure 4(a) represents the theoretical calculations for the isotope $^{292}_{118}\text{Og}$, and it shows that the isotope $^{292}_{118}\text{Og}$ survives fission and produces 5α chains.

The α -decay and the spontaneous fission half-lives for the isotopes $^{293}_{118}\text{Og}$ and $^{294}_{118}\text{Og}$ are displayed in Figs. 5 and 6(a), respectively. The behavior of α -decay half-lives with increasing mass number of the parent nucleus is almost the same in the two figures. Based on the values of $T_{1/2}^{\text{calc}1}$ and $T_{1/2}^{\text{mB1}}$ present on Table II and shown in Figs. 5 and 6(a), the two isotopes $^{293}_{118}\text{Og}$ and $^{294}_{118}\text{Og}$ survive fission, and the present study predicts 4α and 3α chains from the elements $^{293}_{118}\text{Og}$ and $^{294}_{118}\text{Og}$, respectively. It should be noted that the two α -decay half-lives $T_{1/2}^{\text{calc}1}$ and $T_{1/2}^{\text{mB1}}$ are in good agreement with the experimental data, as shown in Fig. 1. Figure 6(a) shows that we successfully reproduced the decay mode of the element $^{294}_{118}\text{Og}$ which was already synthesized and identified via α decay [2,37] in the laboratory. Thus, we expect that our predictions for the other unknown isotopes of element Og are reliable.

Figures 7–10(a) show the calculations for the isotopes $^{295-298}_{118}\text{Og}$. As the neutron number increases in Og isotopes, the spontaneous fission half-life time decreases. For example, T_{SF} for $^{290}_{118}\text{Og}$ is 1.79×10^{10} s, while for the heavier isotope $^{298}_{118}\text{Og}$ the half-life time of spontaneous fission is $T_{\text{SF}} = 7.22 \times 10^3$ s. Figures 7–10(a) indicate that the isotopes $^{295-298}_{118}\text{Og}$ survive

fission, and 2α chains are predicted from each isotope of $^{295-297}_{118}\text{Og}$ while 1α -chain can be observed from $^{298}_{118}\text{Og}$.

The behavior of the curves representing α -decay half-lives and their rate of variation as the mass number of the parent nucleus decreases are governed by the existence of neutron and proton magic or semimagic numbers. The proton number in all figures varies from $Z_p = 118$ to 104, while the neutron number varies from $N_p = 180$ to 166 in Fig. 10(a) and from $N_p = 172$ to 158 in Fig. 2(a). The magic and semimagic proton numbers in the above range are 116, 114, 108, and 106 [79,80], while the neutron magic numbers in the range 180–158 are 158, 162, 164, 172, and 178 [79,80]. In Fig. 2(a), the maximum value

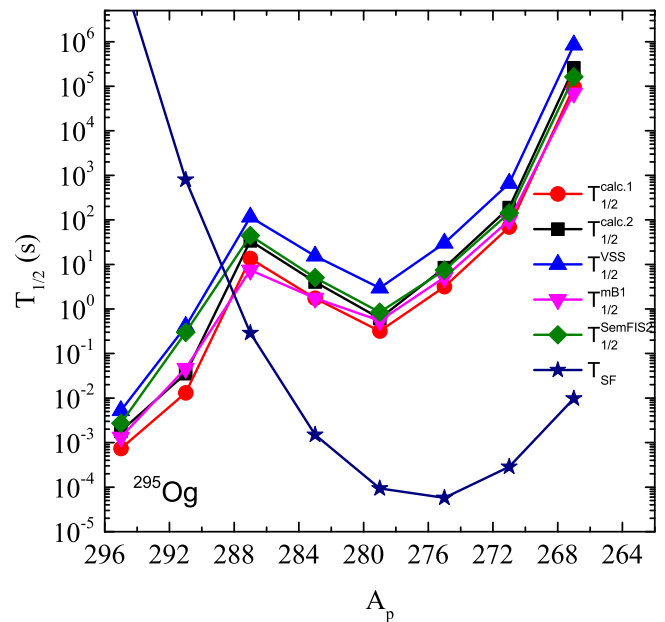


FIG. 7. The same as Fig. 2(a) but for the isotopes $^{295}_{118}\text{Og}$ and products on its α -decay chain.

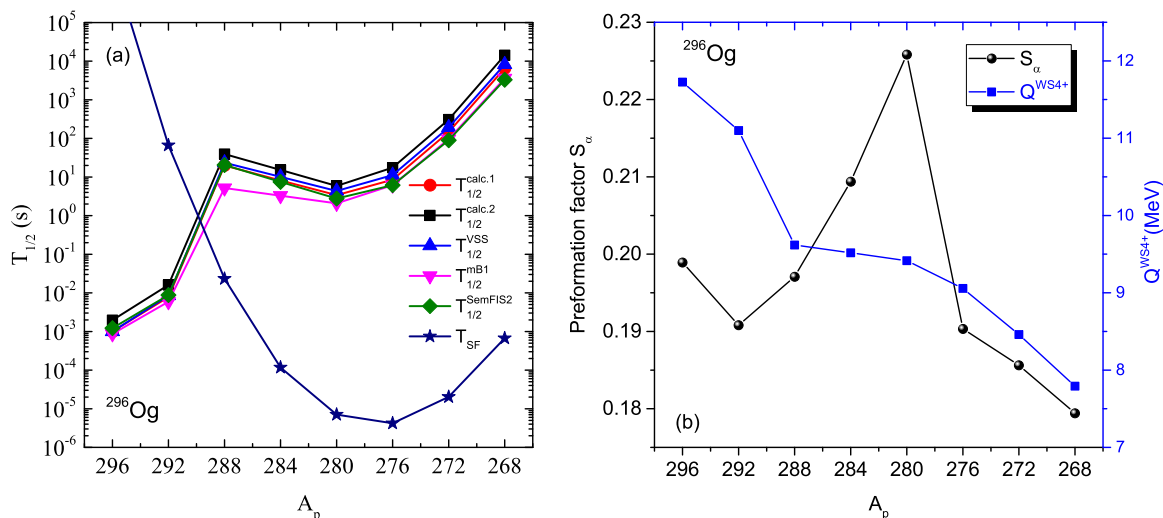


FIG. 8. The same as Fig. 2 but for the isotopes $^{296}_{118}\text{Og}$ and products on its α -decay chain.

of $T_{1/2}$ occurs at $(Z, N) = (116, 170)$, and the rate of variation of $T_{1/2}$ with A_p increases strongly from ^{274}Ds towards the doubly magic nucleus ^{270}Hs . The last two nuclei in Fig. 2(a) are ^{266}Sg and ^{262}Rf ; the first has proton magic number and the second has neutron magic number. Also, in Figs. 3 and 4(a), $T_{1/2}$ increases towards $^{283, 284}\text{Fl}$ and its rate of variation with A_p becomes large towards $^{271, 272}\text{Hs}$ and $^{267, 268}\text{Sg}$, each of which has proton magic number and the neutron number is a magic or near magic number. Concerning Figs. 5–10(a), $T_{1/2}$ for α -decay behaves the same as in Fig. 4(a), except that the last SHN, Rf, has neutron numbers $N_p = 161, 162, 163, 164, 165,$ and 166 , respectively. These numbers are neutron magic or near magic numbers. The neutron numbers $N_p = 162$ and

164 are accompanied by a large degree of stability. This is clear from Figs. 5–10(a): the largest value of $T_{1/2}$ in each of these figures is for the Rf isotopes with $N_p = 161$ –166. $T_{1/2}$ in Figs. 6(a) and 7 increases sharply from Sg to Rf, where the neutron numbers are 162 and 163, respectively. This means that the neutron number $N_p = 162$ has a large degree of stability. Figures 5, 6(a), and 7 show also that $T_{1/2}$ becomes maximum at $Z_p = 114$ for $N_p = 171, 172,$ and 173 , therefore $Z_p = 114$ and $N_p = 172$ show magic character. Figures 8(a), 9, and 10(a) show that the value of $T_{1/2}$ for the four SHN Fl, Cn, Ds, and Hs varies slowly with decreasing A_p . The nuclei show almost the same degree of stability against α decay. The nuclei Fl and Hs have the proton magic numbers 114 and 108, respectively and the two nuclei ^{284}Cn and ^{282}Hs have the neutron magic number 172. The other isotopes of the above mentioned elements have protons or neutrons numbers near magic numbers.

The above discussion of A_p variation of $T_{1/2}$ for α decay of SHN indicates the following:

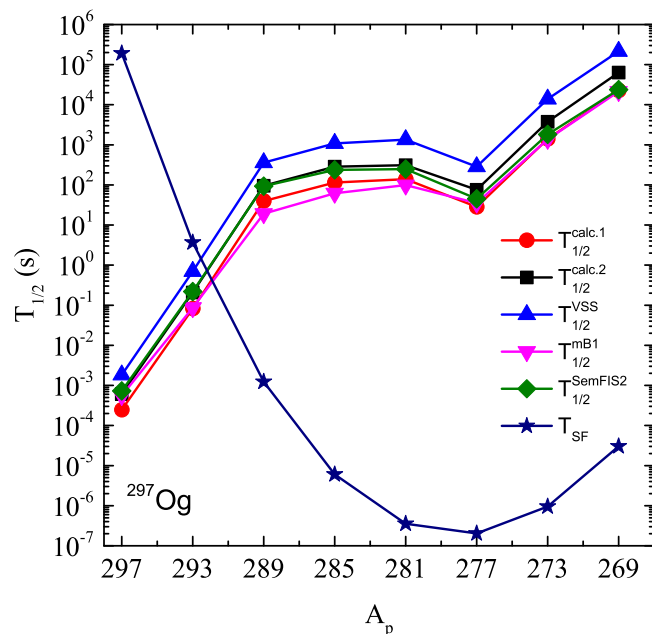


FIG. 9. The same as Fig. 2(a) but for the isotopes $^{297}_{118}\text{Og}$ and products on its α -decay chain.

- (1) The lowest $T_{1/2}$ in each of Figs. 2(a)–10(a) is for the isotopes of superheavy element Og with $N_p = 172$ –180; the $T_{1/2}$ is about 10^{-4} s, which shows that this superheavy element has low degree of stability against α decay. Although the neutron variation range 172–180 has two neutron magic numbers ($N_p = 172$ and 178), they almost fail to increase the stability of the element when combined with proton number $Z_p = 118$.
- (2) As A_p decreases, $T_{1/2}$ increases and reaches a maximum value in Figs. 3–8(a) at $Z_p = 114$ and for neutron numbers varying from 169 to 174. This behavior confirms the proton magic number $Z_p = 114$.
- (3) The value of $T_{1/2}$ is relatively large for α decay of nuclei with $Z_p = 106$ or 108 and $N_p = 162, 164,$ or 172 . Thus the nuclei have high stability against α decay when $Z_p = 106$ or 108 is combined with $N_p = 162, 164,$ or 172 . These neutron and proton numbers were found by other studies and we confirm them in the present study.
- (4) The values of $T_{1/2}$ for the nuclei Sg and Rf, in each of Figs. 2(a), 3, and 4(a), are almost equal. This means that,

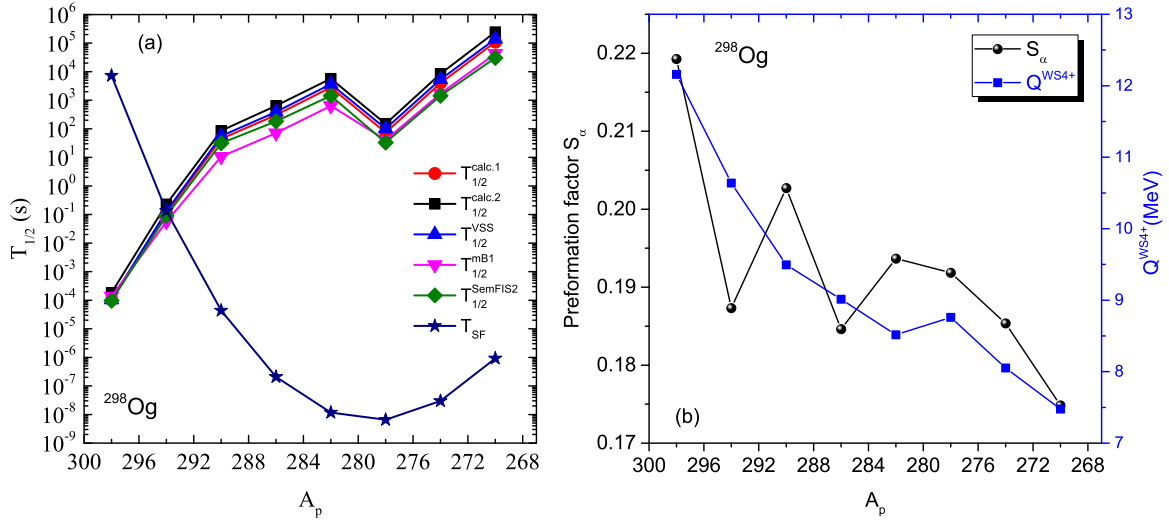


FIG. 10. The same as Fig. 2 but for the isotopes $^{298}_{118}\text{Og}$ and products on its α -decay chain.

for the proton magic number $Z_p = 106$ combined with the number of neutrons $N_p = 160$, the nucleus has the same stability against α decay as $Z_p = 104$ combined with the neutron magic number $N_p = 158$. The same occurs for $(Z_p, N_p) = (106, 161)$ and $(104, 159)$; also $(106, 162)$ and $(104, 160)$.

Thus the study of the behavior of the α -decay half-lives for element Og and its α chains with respect to the mass number of the parent nuclei predicts the proton and neutron numbers at which the SHN will have more stability. We found magic or semimagic numbers consistent with previous studies. In the present study $Z_p = 116, 114, 108,$ and 106 and $N_p = 158, 162, 164, 172,$ and 178 are nucleon numbers associated with large stability compared with others.

To show the correlation between Q_α and T_α and to find any possible correlation between S_α , calculated from the

recently proposed cluster-formation model (CFM), and T_α , we introduce Figs. 2(b), 4(b) 6(b), 8(b), and 10(b). These figures illustrate the variation of the α -preformation factor based on the CFM and the Q value extracted from the recent WS4+ mass model of the even-even isotopes $^{290}_{118}\text{Og}$, $^{292}_{118}\text{Og}$, $^{294}_{118}\text{Og}$, $^{296}_{118}\text{Og}$, $^{298}_{118}\text{Og}$ and their corresponding α -decay chains versus parent mass number A_p . Comparison between Figs. 2(a) and 2(b) shows that the Q -value variation with A_p follows inversely the behavior of T_α with the parent mass number A_p . Large and small Q values correspond respectively, to less and more stability against α decay. The α -particle preformation factor, S_α , is usually calculated as the ratio of the calculated half-life to the experimentally observed value [10]. Recently, the cluster formation model [57,62–64] has been used to calculate S_α independently of the half-lives. Our previous studies [8,9,68] of the variation of S_α with nucleon number indicated that S_α is strongly correlated to magic nucleon numbers and the

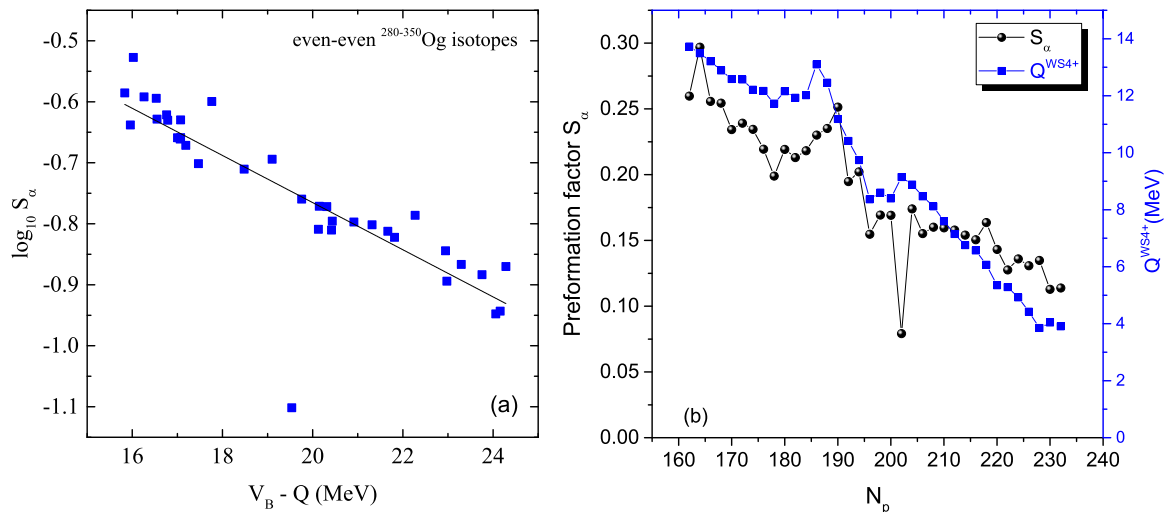


FIG. 11. (a) A negative linear correlation between the logarithm of the α -preformation factor, S_α , and the fragmentation potential (defined as $V_B - Q$) for even-even $^{280-350}_{118}\text{Og}$ isotopes. (b) Variation of the α -preformation factor and the Q value extracted from the recent WS4+ mass model for even-even $^{280-350}_{118}\text{Og}$ isotopes versus parent neutron number N_p .

TABLE III. Comparison of the calculated α -decay half-lives using the cluster formation model (CFM) of the isotope ^{290}Og and its α -decay chain. The half-lives are calculated using the double-folding model based on M3Y-Paris with the finite-range exchange part of the NN interaction (Sph-FR) as well as for zero-range exchange (Sph-ZR) assuming spherical shapes of daughter nuclei. The calculation of half-lives including deformation of the involved nuclei with the zero-range exchange contribution (Def-ZR) are also added for comparison. The Q values and deformation parameters (β_2^d and β_4^d) of the daughter nuclei are extracted from the recent WS4+ mass model [55].

| Parent nuclei | $Q_\alpha^{\text{WS4+}}$ (MeV) | S_α | β_2^d | β_4^d | $T_{1/2}^{\text{Sph-FR}}$ (s) | $T_{1/2}^{\text{Sph-ZR}}$ (s) | $T_{1/2}^{\text{Def-ZR}}$ (s) |
|-------------------------|--------------------------------|------------|-------------|-------------|-------------------------------|-------------------------------|-------------------------------|
| $^{290}_{118}\text{Og}$ | 12.572 | 0.239 | 0.0750 | 0.0036 | 2.85×10^{-5} | 7.71×10^{-5} | 7.13×10^{-5} |
| $^{286}_{116}\text{Lv}$ | 11.280 | 0.218 | -0.0594 | 0.0039 | 6.12×10^{-3} | 1.69×10^{-2} | 1.61×10^{-2} |
| $^{282}_{114}\text{Fl}$ | 11.340 | 0.264 | 0.1653 | -0.0476 | 9.12×10^{-4} | 2.47×10^{-3} | 1.71×10^{-3} |
| $^{278}_{112}\text{Cn}$ | 11.739 | 0.253 | 0.2021 | -0.0640 | 3.10×10^{-5} | 8.16×10^{-5} | 4.92×10^{-5} |
| $^{274}_{110}\text{Ds}$ | 10.896 | 0.222 | 0.2174 | -0.0521 | 7.45×10^{-4} | 1.97×10^{-3} | 1.12×10^{-3} |
| $^{270}_{108}\text{Hs}$ | 9.135 | 0.214 | 0.2280 | -0.0401 | 1.08×10^1 | 2.93×10^1 | 1.50×10^1 |
| $^{266}_{106}\text{Sg}$ | 8.566 | 0.206 | 0.2244 | -0.0243 | 1.46×10^2 | 3.97×10^2 | 2.04×10^2 |
| $^{262}_{104}\text{Rf}$ | 8.431 | 0.204 | 0.2246 | -0.0097 | 7.56×10^1 | 2.03×10^2 | 1.04×10^2 |

degree of stability of parent and daughter nuclei. Its value is also sensitive to the change of sequence of energy levels from which the neutrons and protons of α particles are emitted from parent and daughter nuclei. Since most of the energy level sequences for superheavy nuclei are unknown, we try to correlate the behavior of S_α to change of stability and presence of magic neutron and proton numbers. Figure 2(b) shows that the behavior of S_α , calculated using CFM, and the Q value with A_p are the same except for the nucleus $^{282}_{114}\text{Fl}$ where the value of S_α increases from 0.22 to 0.265. The jump of S_α for the isotope $^{282}_{114}\text{Fl}$ may be attributed to its proton magic number ($Z_p = 114$), which when combined with the neutron number $N_p = 168$ produces a less stable nucleus against α decay. The stability at $Z_p = 114$ is still weak when combined with $N_p = 170$, as shown in Fig. 4(b) for the nucleus $^{282}_{114}\text{Fl}$. Figures 4(b) and 6(b) are the same as Fig. 2(b) except they are for the isotopes $^{292}_{118}\text{Og}$ and $^{294}_{118}\text{Og}$, respectively. The A_p variation of the curves, representing Q value and S_α in the two figures, is almost the same as in Fig. 2(b). The appearance of the neutron magic number $N_p = 172$ combined with proton magic number $Z_p = 114$ causes the nucleus $^{286}_{114}\text{Fl}$ to gain some stability, as shown from the behavior of the S_α curve in Fig. 6(b). Also, the nucleus ^{282}Cn gains stability because its number of neutrons becomes $N_p = 170$ (near a neutron magic number). The behavior of the Q -value curves in Figs. 8(b) and 10(b) follow inversely the behavior of $T_{1/2}$ curves in Figs. 8(a) and 10(a), respectively. For the curves representing S_α , the effect of the neutron magic number $N = 172$ appears to increase slightly the stability of ^{284}Cn in Fig. 8(b), and the stability of ^{282}Ds is increased by about 15% in Fig. 10(b) compared to the isotope ^{280}Ds in Fig. 8(b). The behavior of S_α for the last four points representing nuclei Ds, Hs, Sg, and Rf is consistent with the behavior of the corresponding Q values of these nuclei. As can be seen from Figs. 2(b), 4(b), 6(b), 8(b), and 10(b), the behavior of the preformation factor, calculated using the CFM, and the Q value with the nucleon number are almost consistent.

Figure 11(a) depicts the logarithm of preformation factor S_α extracted from the CFM as a function of the fragmentation (or driving) potential $V_B - Q$, which is defined as the difference between the Coulomb barrier height V_B and

the Q value, for even-even $^{280-350}_{118}\text{Og}$ isotopes. As can be seen from Fig. 11(a), the logarithm of S_α roughly follows a negative linear correlation with the fragmentation potential, which is consistent with the result in Ref. [81] for the reduced width square (proportional to S_α). Therefore, the result in Fig. 11(a) confirms that the obtained S_α is reasonable in its general variation. Figure 11(b) illustrates the variation of both the α -preformation factor and the Q value extracted from the recent WS4+ mass model for even-even $^{280-350}_{118}\text{Og}$ isotopes versus the neutron number N_p values of the parent nuclei. Consistent behavior is seen in Fig. 11(b) for the neutron number variation of the preformation factor, which is obtained from the CFM, and the Q value, which is extracted from the WS4+ mass model. It is worth mentioning that the nucleus $^{320}_{118}\text{Og}$ deviates from the general trend in Figs. 11(a) and 11(b). This may be attributed to small formation energy, Eq. (19), for such an isotope compared to its neighbors: consequently a sudden

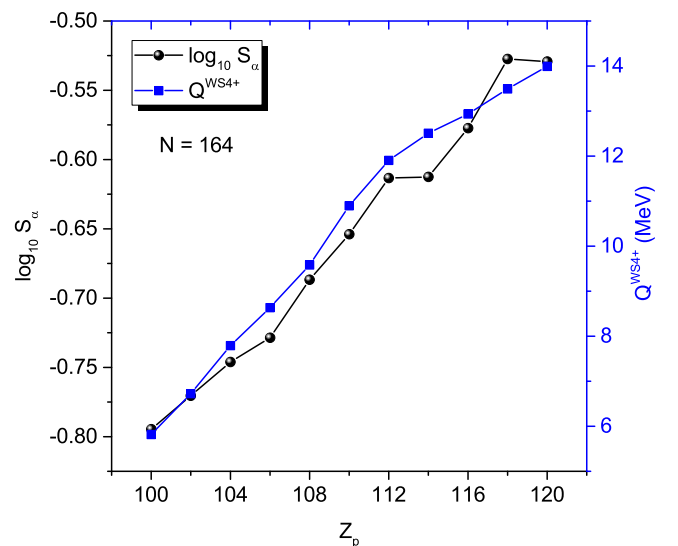


FIG. 12. The variation of the logarithm of the α -preformation factor and the Q values with the proton number of α emitters for even-even nuclei in the $N = 164$ isotonic chain.

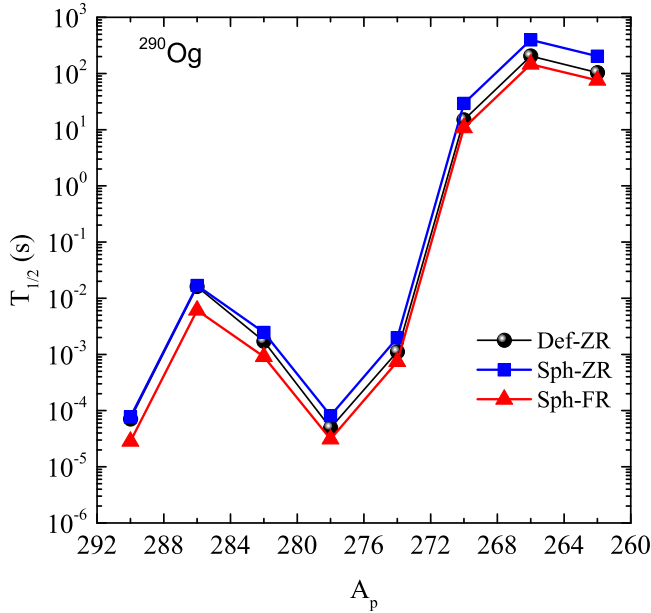


FIG. 13. Comparison of the calculated α -decay half-lives using the cluster formation model (CFM) of the isotope $^{290}_{118}\text{Og}$ and its α -decay chain. The half-lives are calculated using the double-folding model based on M3Y-Paris with the finite-range exchange part of the NN interaction (Sph-FR) as well as for zero-range exchange [59] (Sph-ZR) assuming spherical shapes of daughter nuclei. The calculation of half-lives with including deformation of the involved nuclei with the zero-range exchange contribution (Def-ZR) are also added for comparison.

decrease in the α -preformation factor occurs which means that this isotope shows enhanced stability against α decay.

In order to obtain a better insight, the logarithm of the α -preformation factor, $\log_{10} S\alpha$, and the Q value are plotted versus the proton number of the parent nucleus in Fig. 12 for even-even isotones with $N_p = 164$. It can be clearly seen from Fig. 12 that there exist Z -dependent linear relations for both $\log_{10} S\alpha$ and the Q value. This confirms the correlation between Q value and $S\alpha$.

Finally, to explore the effect of deformation and orientation degrees of freedom on the α -decay half-lives, we have incorporated deformation effects up to hexadecapole deformation for the calculation of the α -decay half-lives for the element $^{290}_{118}\text{Og}$ and its α -decay chain using the M3Y-Paris NN interaction with zero-range (ZR) exchange forces. The quadrupole (β_2^d) and hexadecapole (β_4^d) deformation parameters are extracted from the WS4 mass model [55]. The methods of calculating the knocking frequency, the penetration probability, and the half-lives are outlined in Refs. [30,59]. We have used the α -preformation factor calculated from the CFM. Our results for α -decay half-lives of $^{290}_{118}\text{Og}$ and its α -decay chain both for spherical as well as deformed choices of shapes are reported in Table III and further illustrated in Fig. 13. As can be seen from

Table III and Fig. 13, considering the deformation degrees of freedom of the involved nuclei with the zero-range exchange part of NN interaction reduces the half-life time compared with the zero-range results for spherical nuclei. Deformation is reflected in orientation-angle-dependent nuclear radius, which leads to enhanced penetration for larger radii. Owing to deformed barrier effects, the nuclear deformation mainly affects the barrier penetration probability of the α particle and hence decreases α -decay half-lives. Moreover, the general trends of α -decay half-lives with mass number are identical for both spherical and deformed calculations. Using the finite-range instead of the zero-range exchange NN force does not affect the behavior of $T_{1/2}$ with mass number variation but reduces its value. Deformation of the daughter nucleus reduces the calculated α -decay half-lives by a factor of about 2 or less, compared to the spherical shape.

IV. SUMMARY AND CONCLUSION

The α -decay chains and the mode of decay of the isotopes of the superheavy nuclei with $Z = 118$ within the atomic mass number range $290 \leq A \leq 298$ have been studied within the density dependent cluster model. The double-folding model with realistic NN interaction has been used to calculate the α -nucleus potential which is then used to calculate the α -decay half-lives of nine isotopes of the SHN Og and its decay products. The α -decay preformation factor which measures the probability of formation of an α particle was derived from the recent cluster formation model. We compared our results for the α -decay half-lives with the experimental results for 36 known superheavy nuclei and the half-lives calculated from the three semiempirical formulas VSS [46,47], mB1 [51], and SemFIS2 [53]. The successful manifestation of the experimental α -decay half-lives of the 36 SHN made our study reliable, and thus we aimed at predicting the α -decay chains of some unknown isotopes of element Og. For the nine $^{290-298}_{118}\text{Og}$ isotopes and their decay products, we calculated the α -decay half-lives using five different methods and compared the values with the corresponding half-life times for spontaneous fission. This comparison predicts 5α chains for each of the isotopes $^{290-292}_{118}\text{Og}$, 4α chains for $^{293}_{118}\text{Og}$, 3α chains for $^{294}_{118}\text{Og}$, and 2α chains for $^{295-297}_{118}\text{Og}$. We studied the behavior of the α -decay half-life curves as a function of mass number of parent nuclei and found that this behavior is governed by magic proton and neutron numbers. We have found a linear dependence between the logarithm of the preformation probability and fragmentation potential for even-even $^{280-350}_{118}\text{Og}$ isotopes. Moreover, α -decay half-lives are also calculated by including the deformation effect of the daughter nucleus. Deformation of the daughter nucleus affects the α -decay half-lives typically by a factor of 2 or less, compared to the spherical shape, and does not affect the behavior of α -decay half-lives with respect to mass number.

[1] S. Hofmann and G. Munzenberg, *Rev. Mod. Phys.* **72**, 733 (2000).

[2] Y. T. Oganessian and K. P. Rykaczewski, *Phys. Today* **68**, 32 (2015).

- [3] M. Ismail, A. Adel, and M. M. Botros, *Phys. Rev. C* **93**, 054618 (2016).
- [4] Y. Qian, Z. Ren, and D. Ni, *Phys. Rev. C* **89**, 024318 (2014).
- [5] D. Bucurescu and N. V. Zamfir, *Phys. Rev. C* **87**, 054324 (2013).
- [6] D. Ni and Z. Ren, *Phys. Rev. C* **87**, 027602 (2013).
- [7] D. Ni, Z. Ren, T. Dong, and Y. Qian, *Phys. Rev. C* **87**, 024310 (2013).
- [8] M. Ismail and A. Adel, *Phys. Rev. C* **88**, 054604 (2013).
- [9] M. Ismail and A. Adel, *Nucl. Phys. A* **912**, 18 (2013).
- [10] W. M. Seif, M. Shalaby, and M. F. Alrakshy, *Phys. Rev. C* **84**, 064608 (2011).
- [11] Y. T. Oganessian, F. S. Abdullin, C. Alexander, J. Binder, R. A. Boll, S. N. Dmitriev, J. Ezold, K. Felker, J. M. Gostic, R. K. Grzywacz, J. H. Hamilton, R. A. Henderson, M. G. Itkis, K. Miernik, D. Miller, K. J. Moody, A. N. Polyakov, A. V. Ramayya, J. B. Roberto, M. A. Ryabinin, K. P. Rykaczewski, R. N. Sagaidak, D. A. Shaughnessy, I. V. Shirokovsky, M. V. Shumeiko, M. A. Stoyer, N. J. Stoyer, V. G. Subbotin, A. M. Sukhov, Y. S. Tsyganov, V. K. Utyonkov, A. A. Voinov, and G. K. Vostokin, *Phys. Rev. C* **87**, 054621 (2013).
- [12] Y. T. Oganessian, F. S. Abdullin, P. D. Bailey, D. E. Benker, M. E. Bennett, S. N. Dmitriev, J. G. Ezold, J. H. Hamilton, R. A. Henderson, M. G. Itkis, Y. V. Lobanov, A. N. Mezentsev, K. J. Moody, S. L. Nelson, A. N. Polyakov, C. E. Porter, A. V. Ramayya, F. D. Riley, J. B. Roberto, M. A. Ryabinin, K. P. Rykaczewski, R. N. Sagaidak, D. A. Shaughnessy, I. V. Shirokovsky, M. A. Stoyer, V. G. Subbotin, R. Sudowe, A. M. Sukhov, Y. S. Tsyganov, V. K. Utyonkov, A. A. Voinov, G. K. Vostokin, and P. A. Wilk, *Phys. Rev. Lett.* **104**, 142502 (2010).
- [13] Y. T. Oganessian, V. K. Utyonkov, Y. V. Lobanov, F. S. Abdullin, A. N. Polyakov, R. N. Sagaidak, I. V. Shirokovsky, Y. S. Tsyganov, A. A. Voinov, G. G. Gulbekian, S. L. Bogomolov, B. N. Gikal, A. N. Mezentsev, S. Iliev, V. G. Subbotin, A. M. Sukhov, K. Subotic, V. I. Zagrebaev, G. K. Vostokin, M. G. Itkis, K. J. Moody, J. B. Patin, D. A. Shaughnessy, M. A. Stoyer, N. J. Stoyer, P. A. Wilk, J. M. Kenneally, J. H. Landrum, J. F. Wild, and R. W. Lougheed, *Phys. Rev. C* **74**, 044602 (2006).
- [14] K. P. Santhosh and C. Nithya, *At. Data Nucl. Data Tables* **119**, 33 (2018).
- [15] K. P. Santhosh and C. Nithya, *Eur. Phys. J. A* **53**, 189 (2017).
- [16] K. P. Santhosh and C. Nithya, *Phys. Rev. C* **96**, 044613 (2017).
- [17] K. P. Santhosh and C. Nithya, *Phys. Rev. C* **95**, 054621 (2017).
- [18] K. P. Santhosh and C. Nithya, *Phys. Rev. C* **94**, 054621 (2016).
- [19] K. P. Santhosh and C. Nithya, *Eur. Phys. J. A* **52**, 371 (2016).
- [20] K. P. Santhosh and C. Nithya, *Int. J. Mod. Phys. E* **25**, 1650079 (2016).
- [21] J. P. Cui, Y. L. Zhang, S. Zhang, and Y. Z. Wang, *Phys. Rev. C* **97**, 014316 (2018).
- [22] P. Mohr, *Phys. Rev. C* **95**, 011302(R) (2017).
- [23] S. Zhang, Y. Zhang, J. Cui, and Y. Wang, *Phys. Rev. C* **95**, 014311 (2017).
- [24] Y. Lim and Y. Oh, *Phys. Rev. C* **95**, 034311 (2017).
- [25] X. J. Bao, S. Q. Guo, H. F. Zhang, and J. Q. Li, *Phys. Rev. C* **95**, 034323 (2017).
- [26] C. I. Anghel and I. Silisteanu, *Phys. Rev. C* **95**, 034611 (2017).
- [27] C. Xu, G. Röpke, P. Schuck, Z. Ren, Y. Funaki, H. Horiuchi, A. Tohsaki, T. Yamada, and B. Zhou, *Phys. Rev. C* **95**, 061306(R) (2017).
- [28] S. V. Tolokonnikov, I. N. Borzov, M. Kortelainen, Y. S. Lutostansky, and E. E. Saperstein, *Eur. Phys. J. A* **53**, 33 (2017).
- [29] H. C. Manjunatha and K. N. Sridhar, *Eur. Phys. J. A* **53**, 156 (2017).
- [30] M. Ismail, W. M. Seif, A. Adel, and A. Abdurrahman, *Nucl. Phys. A* **958**, 202 (2017).
- [31] S. Dahmardeh, S. A. Alavi, and V. Dehghani, *Nucl. Phys. A* **963**, 68 (2017).
- [32] Y. L. Zhang and Y. Z. Wang, *Nucl. Phys. A* **966**, 102 (2017).
- [33] N. A. M. Alsaif, S. Radiman, and S. M. S. Ahmed, *J. Phys. G: Nucl. Part. Phys.* **44**, 105103 (2017).
- [34] D. T. Akrawy and D. N. Poenaru, *J. Phys. G: Nucl. Part. Phys.* **44**, 105105 (2017).
- [35] Yu. Ts. Oganessian, A. Sobiczewski and G. M. Ter-Akopian, *Phys. Scr.* **92**, 023003 (2017).
- [36] J. Hong, G. G. Adamian, and N. V. Antonenko, *Phys. Lett. B* **764**, 42 (2017).
- [37] Y. T. Oganessian and V. K. Utyonkov, *Nucl. Phys. A* **944**, 62 (2015).
- [38] A. Sobiczewski, *Phys. Rev. C* **94**, 051302(R) (2016).
- [39] D. Ackermann, *Nucl. Phys. A* **787**, 353 (2007).
- [40] Y. T. Oganessian and V. K. Utyonkov, *Rep. Prog. Phys.* **78**, 036301 (2015).
- [41] K. Morita, *Nucl. Phys. A* **944**, 30 (2015).
- [42] G. Gamow, *Z. Phys.* **51**, 204 (1928).
- [43] H. F. Zhang and G. Royer, *Phys. Rev. C* **76**, 047304 (2007).
- [44] D. N. Poenaru, M. Ivasÿcu, and A. Scandulescu, *J. Phys. G: Nucl. Part. Phys.* **5**, L169 (1979).
- [45] C. Xu and Z. Ren, *Nucl. Phys. A* **753**, 174 (2005).
- [46] V. E. Viola, Jr. and G. T. Seaborg, *J. Inorg. Nucl. Chem.* **28**, 741 (1966).
- [47] A. Sobiczewski, Z. Patyk, and S. Cwiok, *Phys. Lett. B* **224**, 1 (1989).
- [48] D. Ni, Z. Ren, T. Dong, and C. Xu, *Phys. Rev. C* **78**, 044310 (2008).
- [49] G. Royer, *J. Phys. G: Nucl. Part. Phys.* **26**, 1149 (2000).
- [50] A. Sobiczewski and A. Parkhomenko, *Prog. Part. Nucl. Phys.* **58**, 292 (2007).
- [51] A. I. Budaca, R. Budaca, and I. Silisteanu, *Nucl. Phys. A* **951**, 60 (2016).
- [52] M. Horoi, B. A. Brown, and A. Sandulescu, *J. Phys. G: Nucl. Part. Phys.* **30**, 945 (2004).
- [53] D. N. Poenaru, R. A. Gherghescu, and N. Carjan, *Europhys. Lett.* **77**, 62001 (2007).
- [54] Y. Z. Wang, S. J. Wang, Z. Y. Hou, and J. Z. Gu, *Phys. Rev. C* **92**, 064301 (2015).
- [55] N. Wang, M. Liu, X. Z. Wu, and J. Meng, *Phys. Lett. B* **734**, 215 (2014); <http://www.imqmd.com/mass/>
- [56] K. Varga, R. G. Lovas, and R. J. Liotta, *Phys. Rev. Lett.* **69**, 37 (1992).
- [57] S. M. S. Ahmed, R. Yahaya, S. Radiman, and M. S. Yasir, *J. Phys. G: Nucl. Part. Phys.* **40**, 065105 (2013).
- [58] M. Ismail and A. Adel, *Phys. Rev. C* **90**, 064624 (2014).
- [59] M. Ismail and A. Adel, *Phys. Rev. C* **89**, 034617 (2014).
- [60] H. F. Zhang and G. Royer, *Phys. Rev. C* **77**, 054318 (2008).
- [61] D. Ni and Z. Ren, *Phys. Rev. C* **81**, 024315 (2010).
- [62] D. Deng, Z. Ren, D. Ni, and Y. Qian, *J. Phys. G: Nucl. Part. Phys.* **42**, 075106 (2015).
- [63] D. Deng and Z. Ren, *Phys. Rev. C* **93**, 044326 (2016).
- [64] S. M. S. Ahmed, *Nucl. Phys. A* **962**, 103 (2017).
- [65] M. Ismail, F. Salah, and M. M. Osman, *Phys. Rev. C* **54**, 3308 (1996).

- [66] M. Ismail, M. M. Osman, and F. Salah, *Phys. Rev. C* **60**, 037603 (1999).
- [67] D. T. Khoa, *Phys. Rev. C* **63**, 034007 (2001).
- [68] M. Ismail and A. Adel, *Phys. Rev. C* **86**, 014616 (2012).
- [69] G. R. Satchler and W. G. Love, *Phys. Rep.* **55**, 183 (1979).
- [70] M. Ismail, A. Y. Ellithi, M. M. Botros, and A. Adel, *Phys. Rev. C* **81**, 024602 (2010).
- [71] G. Wentzel, *Z. Phys.* **38**, 518 (1926).
- [72] N. G. Kelkar and H. M. Castaneda, *Phys. Rev. C* **76**, 064605 (2007).
- [73] R. E. Langer, *Phys. Rev.* **51**, 669 (1937).
- [74] J. J. Morehead, *J. Math. Phys.* **36**, 5431 (1995).
- [75] D. T. Khoa, W. von Oertzen, and H. G. Bohlen, *Phys. Rev. C* **49**, 1652 (1994).
- [76] N. Anantaraman, H. Toki, and G. F. Bertsch, *Nucl. Phys. A* **398**, 269 (1983).
- [77] M. E. Brandan and G. R. Satchler, *Phys. Rep.* **285**, 143 (1997).
- [78] C. Xu, Z. Ren, and Y. Guo, *Phys. Rev. C* **78**, 044329 (2008).
- [79] M. Ismail, A. Y. Ellithi, A. Adel, and H. Anwer, *J. Phys. G: Nucl. Part. Phys.* **43**, 015101 (2016).
- [80] M. Ismail, A. Y. Ellithi, A. Adel, and H. Anwer, *Chin. Phys. C* **40**, 124102 (2016).
- [81] D. S. Delion, *Phys. Rev. C* **80**, 024310 (2009).